5-2-2018

# Myeloid conditioning with c-kit-targeted CAR-T cells enables donor stem cell engraftment

Yasuyuki Arai

Uimook Choi

Cristina I Corsino

Sherry M Koontz

Masaki Tajima

***See next page for additional authors***

**Authors**
Yasuyuki Arai, Uimook Choi, Cristina I Corsino, Sherry M Koontz, Masaki Tajima, Colin L Sweeney, Mary A Black, Steven A Feldman, Mary C Dinauer, and Harry L Malech

Molecular Therapy
Original Article

# Myeloid Conditioning with c-kit-Targeted CAR-T Cells Enables Donor Stem Cell Engraftment

Yasuyuki Arai,[1] Uimook Choi,[1] Cristina I. Corsino,[2] Sherry M. Koontz,[1] Masaki Tajima,[3] Colin L. Sweeney,[1] Mary A. Black,[4] Steven A. Feldman,[4] Mary C. Dinauer,[5] and Harry L. Malech[1]

[1]Genetic Immunotherapy Section, Laboratory of Clinical Immunology and Microbiology, National Institute of Allergy and Infectious Diseases, NIH, Bethesda, MD 20892, USA; [2]Immune Deficiency Genetics Section, Laboratory of Clinical Immunology and Microbiology, National Institute of Allergy and Infectious Diseases, NIH, Bethesda, MD 20892, USA; [3]Mucosal Immunity Section, Laboratory of Clinical Immunology and Microbiology, National Institute of Allergy and Infectious Diseases, NIH, Bethesda, MD 20892, USA; [4]Surgery Branch, National Cancer Institute, NIH, Bethesda, MD 20892, USA; [5]Department of Pediatrics, Washington University School of Medicine, St. Louis, MO 63110, USA

**We report a novel approach to bone marrow (BM) conditioning using c-kit-targeted chimeric antigen receptor T (c-kit CAR-T) cells in mice. Previous reports using anti-c-kit or anti-CD45 antibody linked to a toxin such as saporin have been promising. We developed a distinctly different approach using c-kit CAR-T cells. Initial studies demonstrated *in vitro* killing of hematopoietic stem cells by c-kit CAR-T cells but poor expansion *in vivo* and poor migration of CAR-T cells into BM. Pre-treatment of recipient mice with low-dose cyclophosphamide (125 mg/kg) together with CXCR4 transduction in the CAR-T cells enhanced trafficking to and expansion in BM (<1%–13.1%). This resulted in significant depletion of the BM c-kit$^+$ population (9.0%–0.1%). Because congenic Thy1.1 CAR-T cells were used in the Thy1.2-recipient mice, anti-Thy1.1 antibody could be used to deplete CAR-T cells *in vivo* before donor BM transplant. This achieved 20%–40% multilineage engraftment. We applied this conditioning to achieve an average of 28% correction of chronic granulomatous disease mice by wild-type BM transplant. Our findings provide a proof of concept that c-kit CAR-T cells can achieve effective BM conditioning without chemo-/radiotherapy. Our work also demonstrates that co-expression of a trafficking receptor can enhance targeting of CAR-T cells to a designated tissue.**

## INTRODUCTION

Hematopoietic stem cell (HSC) transplantation is one of the curative therapeutic options for patients with a variety of inherited disorders of blood cells, including immune deficiencies and hemoglobinopathies.[1–3] In addition, considerable progress has been made toward achieving clinical benefit from autologous HSC *ex vivo* gene therapy for some of these disorders.[3,4] In general, some level of bone marrow (BM) conditioning using chemotherapy and/or radiation is needed to achieve the required engraftment of allogeneic HSC or gene-corrected autologous HSC. There is considerable interest in finding less toxic and more focused approaches to achieve BM conditioning. Promising results have been observed using antibody-based approaches including anti-c-kit (CD117)[5,6] or anti-CD45 antibodies,[7] which directly target HSCs. Results with anti-c-kit antibody were enhanced in combination with anti-CD47 antibody,[8] and those with anti-CD45 antibody were greatly enhanced by conjugation to saporin.[9] Here we explored a related, but distinct, approach in immunocompetent congenic mice using c-kit-targeted chimeric antigen receptor T (c-kit CAR-T) cells to deplete HSCs in BM, thereby enabling donor BM engraftment.

As noted, there is considerable work published about antibody-based approaches targeting either c-kit or CD45 on the surface of HSCs or progenitors.[8,9] C-kit is a dimeric transmembrane receptor tyrosine kinase expressed by HSCs and downstream progenitors,[10] and c-kit-ligand signaling through this receptor is essential for HSC homing, proliferation, adhesion, maintenance, and survival.[11,12] On the other hand, CD45 is a cell surface glycoprotein with tyrosine phosphatase activity expressed exclusively on all hematopoietic cells including HSCs, with the exception of platelets and erythrocytes.[13] CD45 participates in the regulation of lymphocyte activation and maturation, as well as thymic selection.[14]

Rat anti-mouse c-kit monoclonal antibody (ACK2) was first reported in 2007 to achieve targeted reduction in HSCs sufficient to allow donor BM engraftment in Rag2$^{-/-}$ $\gamma c^{-/-}$ immunodeficient mice.[5] For this approach to work in T cell-immunocompetent mice required a modest dose (3 Gy) of total body radiation.[6] Conditioning of immunocompetent mice with c-kit antibody combined with anti-CD47 antibody achieved similar BM conditioning without the need for radiation.[8] In this setting, CD47 antibody worked as a myeloid-specific immune checkpoint inhibitor (CD47 acting as a phagocyte "don't eat me" signal[15]). Unmodified anti-CD45 antibody also required radiation (8 Gy) to achieve effective transplant of allogeneic donor HSCs.[7] However, anti-CD45 antibody conjugated with saporin, a

Received 20 December 2017; accepted 5 March 2018;
https://doi.org/10.1016/j.ymthe.2018.03.003.

**Correspondence:** Harry L. Malech, MD, Genetic Immunotherapy Section, Laboratory of Clinical Immunology and Microbiology, National Institute of Allergy and Infectious Diseases, NIH, Building 10, Room 5-3750, 10 Center Dr. MSC1456, Bethesda, MD 20892, USA.
**E-mail:** hmalech@nih.gov

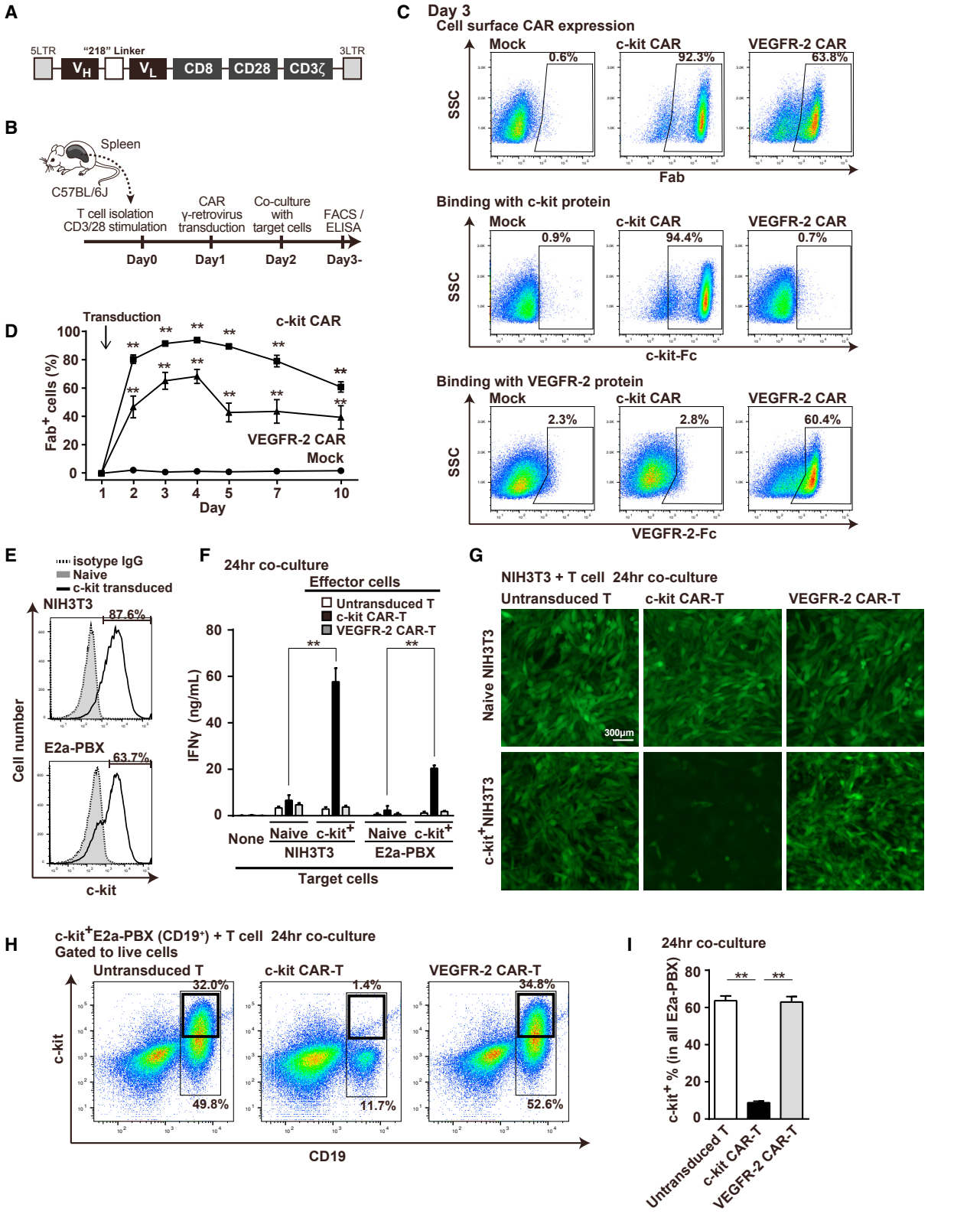


*(legend on next page)*

catalytic N-glycosidase ribosome-inactivating protein that halts protein synthesis,[16] effectively depleted HSCs to achieve a high level of congenic donor engraftment in immunocompetent mice without the need for radiation.[9] While additional stepwise improvements of these antibody-conditioning approaches alone may achieve the ultimate clinical goal of effective BM conditioning without use of any radiation or high-dose chemotherapies, the goal for our study was to explore a related novel approach to BM conditioning using CAR-T cells. If we could demonstrate a proof of concept that CAR-T cells that target HSCs can achieve effective BM conditioning with enhanced donor HSC engraftment, this would add to the list of tools for further development that investigators could apply to this important problem.

CARs are synthetic receptors that target T cells to a specific antigen and reprogram their function.[17,18] CAR-T cells bind surface molecules of target cells through their extracellular antigen-binding domain (antibody element), leading to activation of target cell cytotoxicity via the CAR cytosolic CD3ζ domain independently of engagement of the major histocompatibility complex.[19] CAR-T cell studies are rapidly advancing the field of cancer immunotherapy, especially for acute lymphoblastic leukemia[20] and multiple myeloma.[21] The virtues of CAR-T cells are that the cytotoxicity depends directly on the T cell function, not requiring antibody-mediated activation of macrophages or phagocytes,[22] and that CAR-T cells autonomously expand *in vivo* to magnify the therapeutic effect.[23] These characteristics may be advantageous in the use of this method for BM conditioning, though this approach also requires a means to remove or inactivate the c-kit CAR-T cells to achieve subsequent donor engraftment. In this paper, we show how to achieve efficient BM stem cell depletion and subsequent syngeneic donor engraftment using c-kit CAR-T cells.

## RESULTS

### Specific Cytotoxicity of c-kit CAR-T Cells against c-kit$^+$ Cell Lines *In Vitro*

Immunoglobulin heavy- and light-chain variable region ($V_H$ and $V_L$) of mouse c-kit antibody was connected by 218 linker and inserted into a second-generation CAR γ-retrovirus vector construct[24] (Figure 1A). C57BL/6J mouse T cells were transduced with c-kit CAR vector and analyzed per the schema shown in Figure 1B. Fluorescence-activated cell sorting (FACS) analyses performed 48 hr after retroviral transduction (day 3) demonstrated that >90% of T cells expressed c-kit CAR, as determined by cell surface Fab expression (Figure 1C, top row, middle panel). As a control, we used a previously described vascular endothelial growth factor receptor (VEGFR)-2 CAR vector,[24] which generated >60% of T cells with VEGFR-2 CAR expression (Figure 1C, top row, right panel). Specificity of the CAR-T cells was demonstrated by showing that recombinant c-kit or VEGFR-2 protein bound specifically to its respective CAR-T cell construct. The recombinant c-kit protein conjugated with Fc was detected with anti-Fc fluorescent antibody, and it showed specific binding of c-kit CAR-T cells (Figure 1C, middle row, middle panel). The recombinant VEGFR-2 protein conjugated with Fc was also detected with anti-Fc fluorescent antibody, and it showed specific binding of VEGFR-2 CAR-T cells (Figure 1C, lower row, right panel). We explored alternate constructions of c-kit CAR extracellular antibody domain, varying the order of $V_H$ and $V_L$ and comparing 218[24] versus $(G_4S)_3$ linkers,[25] finding empirically that the $V_H$-218-$V_L$ construct was most efficient at transduction and expression (Figure S1). Furthermore, a more detailed time course analysis of CAR expression detected by anti-Fab (Figure 1D) showed that c-kit CAR or control VEGFR-2 CAR was detected within 24 hr after the retrovirus vector transduction with sustained high expression through day 5, followed by only a modest decrease in the number of cells expressing CAR through day 10 *in vitro*.

We evaluated *in vitro* cytotoxicity of c-kit CAR-T cells toward both adherent (NIH 3T3 murine fibroblast) and suspension (murine B cell leukemia E2a-PBX [CD19$^+$]) cell lines that had been transduced three times with lentivector encoding murine c-kit cDNA to achieve strong surface expression of c-kit in a significant proportion of cells within the target lines (Figure 1E, upper panel and lower panels, respectively). The NIH 3T3 cells (both c-kit$^-$ naive and c-kit$^+$) were also transduced with lentivector encoding GFP to facilitate microscopy visualization of live attached cells. When c-kit$^+$-transduced cell line targets were co-cultured with c-kit CAR-T cells, c-kit CAR-T cell binding to c-kit induced activation-mediated generation of interferon (IFN)γ by the CAR-T cells, as detected in supernatant at 24 hr (two highest bars seen in Figure 1F). Control CAR-T cell cultures with no target cells present (none), with target cells not transduced to express c-kit (naive), with use of untransduced T cells, or with VEGFR-2 CAR-T cells generated little or no IFNγ (Figure 1F). Not shown but previously published is that VEGFR-2 CAR-T cells produce high levels of IFNγ when incubated with cell lines expressing VEGFR-2.[24] Cytotoxicity of c-kit CAR-T cells toward the adherent GFP$^+$c-kit$^+$ NIH 3T3 target in co-culture was visually confirmed by demonstrating detachment of this target cell

**Figure 1. Generation and Evaluation of c-kit CAR-T Cells**

(A) Schematic map of c-kit CAR γ-retrovirus. (B) Timeline of CAR-T cell production and evaluation. (C) FACS analysis (day 3) of c-kit or VEGFR-2 CAR expression detected by anti-murine Fab (top row). Specific binding of Fc-conjugated murine c-kit or VEGFR-2 with c-kit CAR or VEGFR-2 CAR was detected with anti-Fc fluorescent antibody (middle and bottom rows). (D) Time course of c-kit or VEGFR-2 CAR expression (mean ± SD; n = 5; **p < 0.01 compared with mock-transduced T cells). (E) FACS analysis of c-kit expression on NIH 3T3 or E2a-PBX (CD19$^+$) transduced with c-kit lentivector compared to naive. (F) Generation of IFNγ from c-kit CAR-T cells co-cultured with target lines expressing recombinant murine c-kit (mean ± SD; n = 5; **p < 0.01 comparison as indicated). (G) GFP photomicroscopy images of GFP$^+$ NIH 3T3 (naive or c-kit transduced) co-cultured 24 hr with T or CAR-T cells as indicated after PBS rinse. (H) FACS analysis at 24-hr co-culture assessing cytotoxicity of c-kit CAR-T cells toward c-kit$^+$ E2a-PBX that express CD19. Controls include naive T- or VEGFR-2 CAR-T cells. (I) Percentage of the c-kit$^+$ E2a-PBX within the total E2a-PBX remaining at 24 hr in the cytotoxicity co-cultures, as described for (H) (n = 5; mean ± SD; **p < 0.01).

line from the culture plate at 24 hr (Figure 1G, bottom row, middle panel). Control incubations in all the other panels of Figure 1G showed no cytotoxicity detachment. Cytotoxicity of c-kit CAR-T cells toward c-kit$^+$ E2a-PBX cells resulted in lysis, as indicated by the loss of these c-kit$^+$CD19$^+$ target cells from the culture as assessed by FACS at 24 hr (Figure 1H, middle panel, and Figure 1I, middle bar). These c-kit$^+$CD19$^+$ E2a-PBX target cells remained intact in control co-cultures containing untransduced T cells or VEGFR-2 CAR-T cells (Figure 1H, left and right panels, and Figure 1I, left and right bars, respectively). The larger thin line boxes in the Figure 1H panels show the percentage of E2a-PBX in culture, and smaller thick line boxes show the percentage of total culture that are c-kit$^+$ E2a-PBX. The FACS analysis in Figure 1H is a representative experiment where the average of 5 experiments is shown in Figure 1I, where the values indicated for each bar are calculated for each experiment as the proportion (in percent) of (c-kit$^+$ E2a-PBX)/(total E2a-PBX) present after co-culture.

### *In Vitro* Depletion of c-kit$^+$ Population in BM Cells and Inhibition of Colony Formation in Co-culture with c-kit CAR-T Cells

We next assessed c-kit CAR-T cell cytotoxicity toward mouse BM cells *in vitro* using T cells and BM from syngeneic C57BL/6J differing in Thy1 isotype (Thy1.1$^+$ versus Thy1.2$^+$), as indicated in Figure 2A. FACS analysis shows that about 11% of untreated (naive) C57BL/6J BM were c-kit$^+$ (Figure 2B), and it is known that HSC and progenitors were in this population[8] and were mainly CD3 low or negative. Thy1.1$^+$ naive T cells, c-kit CAR-T cells, or VEGFR-2 CAR-T cells were incubated with Thy1.2$^+$ BM in the co-culture assay of IFNγ shown in Figure 2C. The number of BM cells was the same in each culture, but each group differed in the number of T or CAR-T cells (highest to lowest ratios of T cells relative to BM cells). High levels of IFNγ production proportional to the number of c-kit CAR-T cells in the culture were detected in the supernatant at 24 hr of incubation (Figure 2C). Controls (naive T and VEGFR-2 CAR-T cells) as indicated in Figure 2C generated little to no IFNγ.

For the same co-culture experiments in which we assessed IFNγ generation, we also assessed depletion of the BM c-kit$^+$ population at 24 hr by FACS analysis (gating on Thy1.2 as shown in Figures 2D and 2E). At a 1:1 ratio in the culture of Thy1.1 c-kit CAR-T cells with Thy1.2 BM, there was a significant decrease in the BM c-kit$^+$ population from 11.6% to 2.1% (Figure 2D, left and middle panels). Inspection of the Figure 2D middle panel dot plot shows almost total depletion of the cells with high expression of c-kit, where the mean fluorescence intensity (MFI) of the remaining c-kit$^+$ cells was significantly lower than the baseline. Total cell viability in the culture dishes was decreased from 74.9% to 56.7%, which indicated that c-kit CAR-T cells were also damaged after interaction with c-kit$^+$ BM cells (Figure 2D, left and middle panels). The amount of decrease of c-kit$^+$ population was dose dependent on the ratio of BM:c-kit CAR-T cells in the culture (Figure 2E, middle panel). Co-culture controls using untransduced or VEGFR-2 CAR-T cells had no effect on the BM c-kit$^+$ population at 24 hr of co-culture (Figures 2D and 2E, left and right panels or bar sets, respectively).

We next assessed BM colony formation under conditions permissive of myeloid, erythroid, megakaryocyte, and mixed colony formation. Pictures shown in Figure 2F are representative colony plate images from the co-cultures of 1:1 BM:T (or CAR-T cells), where cells were plated at 24 hr co-culture and assessed 10 days later. No colonies were evident in the 1:1 BM:c-kit CAR-T cells co-culture plate (Figure 2F, middle panel), but they are evident in the controls (untransduced T or VEGFR-2 CAR-T cells). When multiple experiments (n = 5) were performed and individual colonies counted, it can be seen that there was a dose-response effect with respect to the ratio of BM:c-kit CAR-T cells in the co-culture and that neither untransduced T cells nor VEGFR-2 CAR-T cells had any effect on colony formation (Figure 2G). At the lower ratios of c-kit CAR-T cells where some colony formation occurred, the specific ratio of myeloid, erythroid, megakaryocyte, and mixed colony formation appeared to be similar to control (data not shown).

### Expansion and Trafficking of c-kit CAR-T Cells in BM after *In Vivo* Injection

After confirming the specificity and intensity of cytotoxicity of c-kit CAR-T cells toward c-kit$^+$ HSCs or progenitor cells *in vitro*, we performed experiments *in vivo* using congenic mouse models to determine expansion and trafficking of c-kit CAR-T cells as per the timeline in Figure 3A. To assess trafficking by whole-body imaging, CAR-T cells were generated from luciferase transgenic mice. Specifically, spleen T cells harvested and CD3 purified from Thy1.1$^+$CD45.2$^+$luciferase$^+$ transgenic C57BL/6J mice were transduced to produce c-kit CAR-T cells, and $5.0 \times 10^6$ of these cells were injected via tail vein into Thy1.2$^+$CD45.2$^+$ C57BL/6J mice. Preliminary studies (data not shown) indicated very poor expansion of CAR-T cells overall and very little trafficking to BM when c-kit CAR-T cells were injected without any other maneuvers. Based on both previous mouse studies with CAR-T cells[26,27] and on human clinical trials using CAR-T cells,[20,21] pre-treatment with a T cell-depleting agent such as cyclophosphamide (CY) appears to be required to achieve expansion and efficient targeted action of CAR-T cells. Preliminary to assessing the effect of CY pre-treatment on CAR-T cell expansion or trafficking, we confirmed that doses of CY up to 250 mg/kg did not appear to have a measurable effect on the mouse BM c-kit$^+$ population or on primitive long-term repopulating hematopoietic cells known as KSL (c-kit$^+$ sca1$^+$Lineage$^-$) that include the most primitive HSC (Figure S2A, top row).

Using this information, we conducted a series of experiments following the scheme shown in Figure 3A, where day −1 was harvest and purification of spleen T cells; day 0 was transduction of T cells and intraperitoneal (i.p.) injection of CY; and day 1 was intravenous (i.v.) injection of c-kit CAR-T cells followed by evaluations of peripheral blood (PB) count, BM FACS, BM histology, BM colony formation, and luciferase whole-body imaging on the indicated days. In initial experiments assessing different dosages of CY pre-treatment, we found that at least 125 mg/kg was needed to achieve optimal expansion of CAR-T cells *in vivo*, but higher doses did not increase

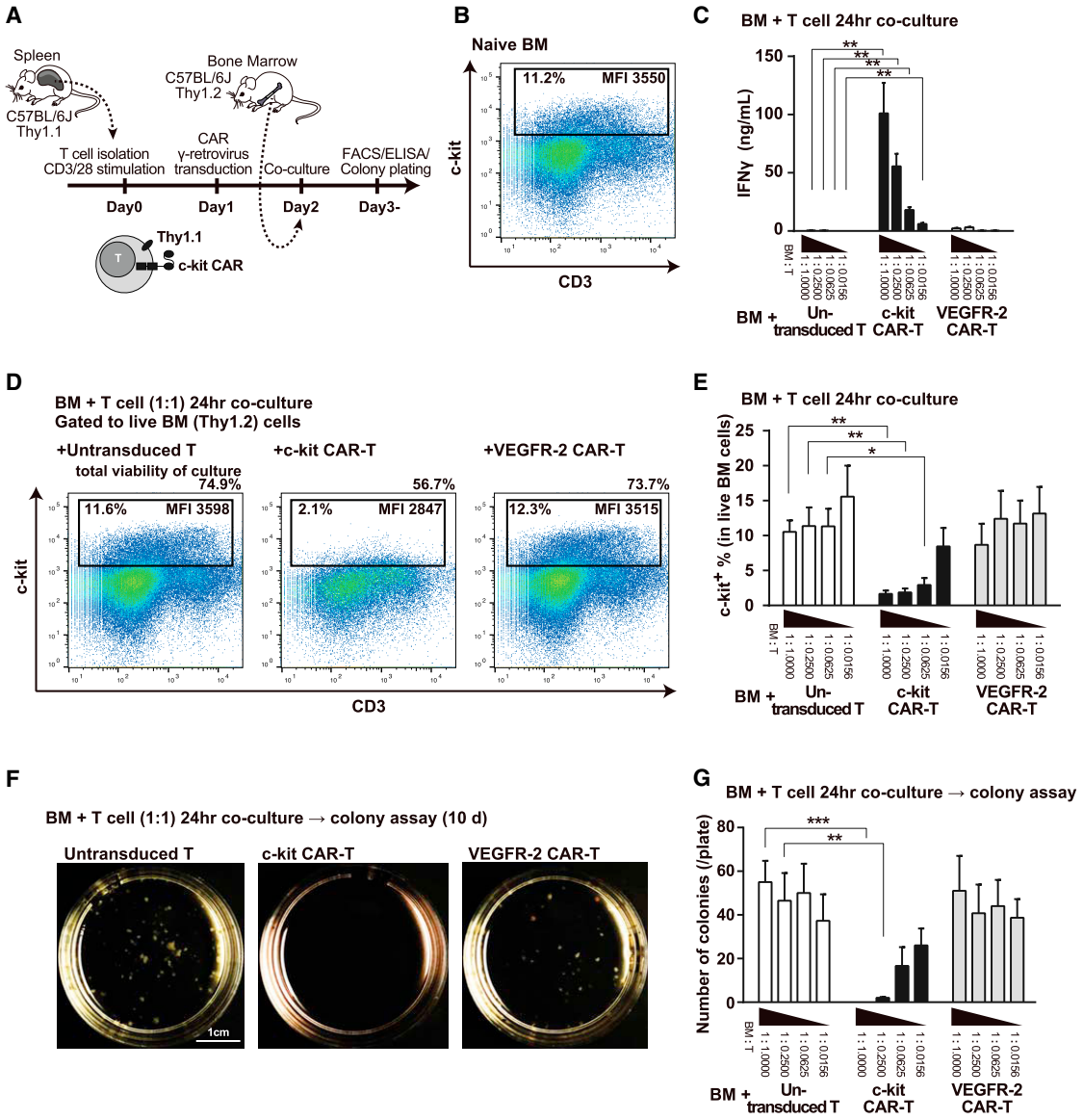


**Figure 2. Congenic Thy1.1 c-kit CAR-T Cell-Mediated Depletion of HSC from Thy1.2 BM *In Vitro***

(A) Timeline of CAR-T production and effect on Thy1.2 BM *in vitro*. (B) FACS analysis of c-kit$^+$ cells in BM. (C) IFNγ secretion by Thy1.1 T or CAR-T cells in 24-hr co-culture at decreasing cell ratios with Thy1.2 BM (n = 5; mean ± SD; **p < 0.01). (D) FACS analysis assessment of Thy1.1 c-kit CAR-T cell-mediated depletion of c-kit$^+$ Thy1.2 BM cells in 1:1 cell ratio co-culture at 24 hr. Percentge of total cell viability in the culture dishes, percentage of c-kit$^+$ cells in BM population, and their mean fluorescence intensity (MFI) are shown in each panel. (E) Summary results of FACS analyses of the same cytotoxicity co-culture as (D), but at different ratios of T cells to BM (n = 5; mean ± SD; **p < 0.01 and *p < 0.05). (F) Photograph of colony formation assays following Thy1.1 c-kit CAR-T cell-mediated depletion of c-kit$^+$ Thy1.2 BM cells in 1:1 cell ratio co-culture that was plated at 24 hr and read at 10 days. (G) Colony formation numbers in the same experimental conditions and analysis as (F) but at different ratios of T cells to BM (n = 5; mean ± SD; ***p <0.001 and **p < 0.01).

this effect (Figure S2A, middle row). Except where specifically indicated, CY (125 mg/kg) was used in subsequent experiments. In the studies shown in Figure 3B, the c-kit CAR-T cells generated from Thy1.1 mice transgenic for luciferase were used. At day 8 after injection of these luciferase$^+$ Thy1.1 c-kit CAR-T cells, the recipient mice were injected with luciferin (3 mg/mouse) i.p. and subjected to whole-body luminescence emission. Emission above the baseline level of detection was only observed in mice prepared with CY and injected with the luciferase transgenic c-kit CAR-T cells (Figure 3B; Figure S3). Despite expansion of the luciferase transgenic c-kit CAR-T cells sufficient to see the luciferase signal, most of the signal was in the region of the spleen and not in regions expected for BM. Shown in later experiments below, despite the CY-mediated overall expansion of the c-kit CAR-T cells mainly in the spleen, there was still insufficient

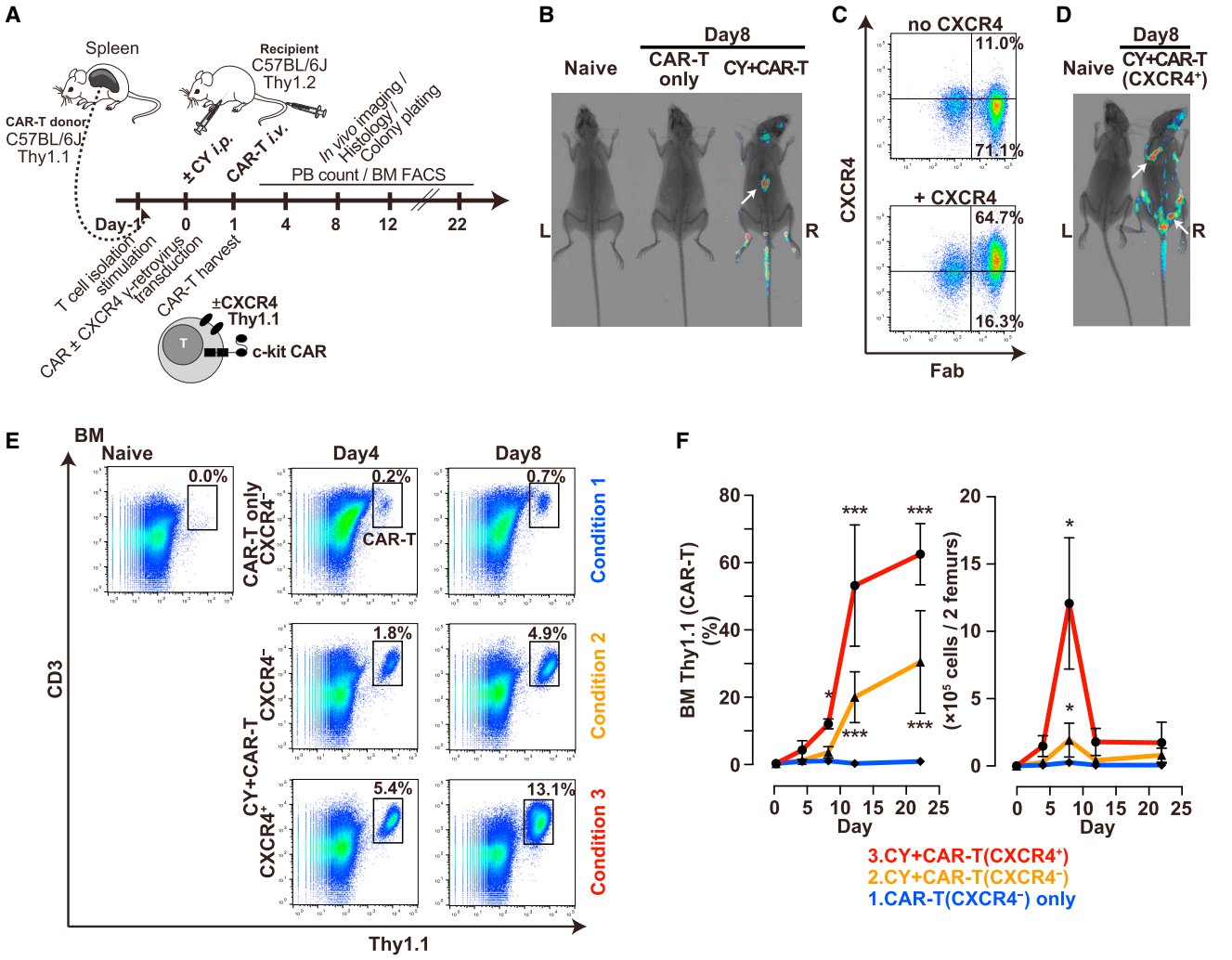


**Figure 3. Trafficking and Expansion of Thy1.1 c-kit CAR-T Cells in Thy1.2 Mice**

(A) Timeline of Thy1.1 CAR-T cell production, *in vivo* administration, expansion, and trafficking. (B) *In vivo* whole-body luciferase luminescence imaging overlaid on X-ray image at day 8 following injection of luciferase$^+$ T (or CAR-T) cells with or without CY pre-treatment, where white arrow indicates spleen. Additional mice are shown in Figure S3. (C) FACS analysis of CXCR4 and c-kit CAR on T cells transduced with c-kit CAR alone (upper panel) or co-transduced with CXCR4 (lower panel). (D) *In vivo* whole-body luciferase luminescence imaging overlaid on X-ray image at day 8 following tail vein injection of luciferase$^+$ CXCR4$^+$ c-kit CAR-T cells into CY-pre-treated mice (right image). White arrows show sites suggestive of BM activity. Additional mice are shown in Figure S3. (E) FACS detection in BM of c-kit CAR or CXCR4$^+$ c-kit CAR-T cells without or with CY pre-treatment as indicated at days 4 and 8 after CAR-T cell administration. (F) Time course of changes in percent (left panel) and actual cell numbers (right panel) of c-kit CAR-T cells in BM using the same conditions as indicated in (E) (n = 5; mean ± SD; ***p <0.001 and *p < 0.05).

trafficking to BM and significantly delayed effect on the BM c-kit$^+$ population.

CXCR4 is a chemokine receptor that regulates leukocyte trafficking and in particular is important for trafficking to and adhesion within BM.[28,29] Though T cells do express low amounts of CXCR4, we explored the forced higher expression of CXCR4 in c-kit CAR-T cells by transduction with γ-retrovirus encoding murine CXCR4 cDNA (Figure 3C) as a means of inducing enhanced migration to and retention in BM. Administration of c-kit CAR-T cells with transduction-mediated overexpression of CXCR4 (CXCR4$^+$ c-kit CAR-T cells) following CY pre-treatment of the mice significantly altered the pattern of luciferase luminescence in the whole-body imaging studies, such that the majority of signal switched from spleen to sites suggestive of improved trafficking to BM (Figure 3D; Figure S3). This conclusion was supported by specific FACS studies of BM outlined next.

BM cells harvested from the Thy1.1$^+$ c-kit CAR-T cell-injected mice were subjected to FACS analysis in order to evaluate the expansion and migration of the Thy 1.1$^+$ c-kit CAR-T cells in a quantitative manner, exploring both the effect of CY pre-treatment and the effect

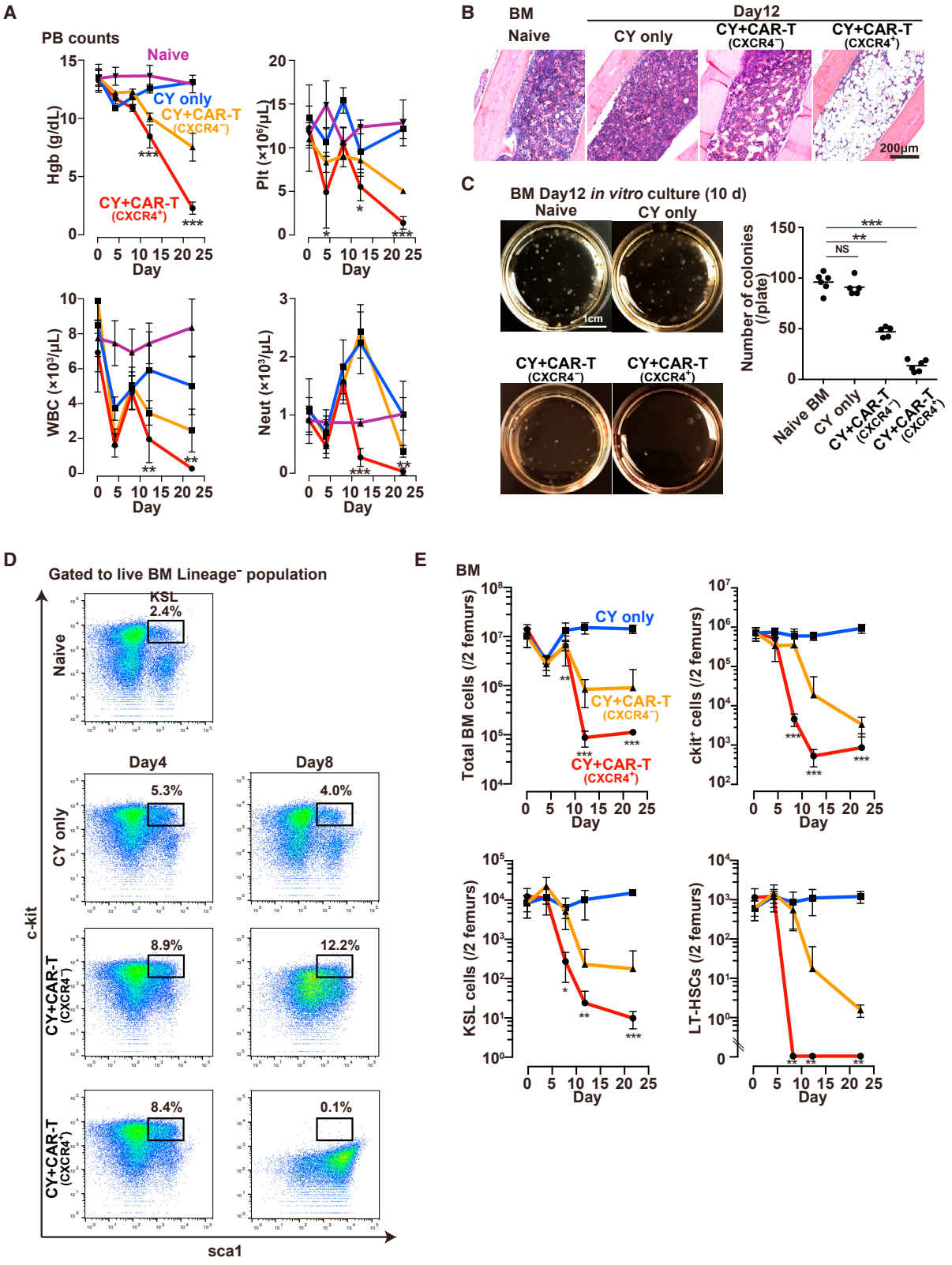


*(legend on next page)*

of CXCR4 co-transduction during generation of the CAR-T cells. Three conditions were compared: (1) injection of c-kit CAR-T cells without CY pre-treatment, (2) injection of c-kit CAR-T cells with CY pre-treatment, and (3) injection of $CXCR4^+$ c-kit CAR-T cells with CY pre-treatment. In the representative FACS dot plot analyses shown in Figure 3E, the condition without forced expression of CXCR4 and without CY pre-treatment (condition 1, upper row) resulted in low levels of migration to BM; the condition without forced expression of CXCR4 but with CY pre-treatment did increase the number of c-kit CAR-T cells in BM (condition 2, middle row); and the combination of forced expression of CXCR4 and CY pre-treatment resulted in the highest level of entry of these $CXCR4^+$ c-kit CAR-T cells into BM (condition 3, bottom row). Naive mouse BM without CY or CAR-T cell treatment is shown at the upper left side of Figure 3E. The time course of each of the three conditions tested over several experiments (n = 5) is shown in Figure 3F (left panel, percentage of CAR-T cells in BM), where there is a >50-fold difference between condition 1 and condition 3 and slightly more than a 2-fold difference between condition 2 and condition 3. Actual numbers of CAR-T cells in the BM (per 2 femurs) are also displayed in Figure 3F (right panel). The apparent substantial increase of percentage of c-kit CAR-T cells in the BM at day 12 and later was in large part due to a significant reduction of total BM cells, as shown below. Based on these observations, all subsequent studies (unless noted) were performed with T cells transduced to express both c-kit CAR and CXCR4, and mouse recipients of these $CXCR4^+$ c-kit CAR-T cells were pre-treated 1 day before with CY at 125 mg/kg.

### Depletion of BM Cells after *In Vivo* Injection of c-kit CAR-T Cells

We next explored the effect of CY conditioning alone or CY conditioning plus $CXCR4^+$ c-kit CAR-T cell treatment on PB counts (Figure 4A), BM cellularity (Figure 4B), BM colony formation (Figure 4C), and the percent and absolute number of the BM KSL ($c\text{-}kit^+sca1^+Lineage^-$) primitive stem cell population (Figures 4D and 4E). Since these mice were not given any BM transplant, the administration of CY conditioning plus $CXCR4^+$ c-kit CAR-T induced anemia, thrombocytopenia, leukopenia, and absolute neutropenia (Figure 4A, red), becoming so severe that most of the mice did not survive more than 5 weeks. Controls receiving only CY (125 mg/kg) without CAR-T cells did not become anemic, thrombocytopenic, or neutropenic, though the total leukocyte count (white blood cell [WBC]) did briefly drop following endogenous T cell depletion by CY (Figure 4A, blue). CY conditioning plus $CXCR4^-$ c-kit CAR-T resulted in less severe and slowly progressing pancytopenia than $CXCR4^+$ c-kit CAR-T (Figure 4A, orange). Histological analyses of BM were performed on day 12 using intact tibia of each mouse that was fixed, decalcified, sectioned, and stained with H&E (Figure 4B). Sections of tibia BM obtained from mice treated with CY+ $CXCR4^+$ CAR-T was remarkably hypo-cellular (Figure 4B, right panel), while BM from mice treated with CY alone or CY+$CXCR4^-$ c-kit CAR-T was unchanged or in milder hypoplasia compared to the naive BM (Figure 4B, the second and third panels, respectively). As expected from the severe pancytopenia and hypocellular BM produced by treatment with CY plus $CXCR4^+$ c-kit CAR-T cells, the colony-forming capacity of BM in those mice was severely depleted relative to either naive or CY only-treated mice (Figure 4C).

The same BM samples were assessed for specific depletion of $c\text{-}kit^+$ and KSL cells (Figures 4D and 4E), total BM cells (Figure 4E), and those KSL cells that were also $CD34^-CD135^-$ (phenotype of long-term repopulating [LT] HSCs) (Figure 4E). The CY only-mediated depletion of T cells resulted in a transient modest decrease in total BM cells at day 4 with recovery thereafter, but no effect on absolute counts of $c\text{-}kit^+$, KSL, or LT-HSC populations in the BM (Figure 4E). In the CY+$CXCR4^+$ c-kit CAR-T condition, by day 8 or beyond there was a several log decrease in absolute count of $c\text{-}kit^+$ cells (Figure 4E, top right panel), absolute count of KSL cells (Figure 4E, bottom left panel), and absolute count of LT-HSCs (Figure 4E, bottom right panel) in BM, with the earliest and most severe depletion observed in the LT-HSC population. Even the total BM nucleated cell count was greatly decreased by day 12 (Figure 4E, top left panel). When we performed the experiment using CY+$CXCR4^-$ c-kit CAR-T, LT-HSC depletion did occur but was substantially delayed in both time of onset and amount of this depletion (Figure 4E, orange). Also of note is that these data from all the sections of Figure 4 again show that CY treatment at 125 mg/kg does not itself cause either PB cytopenia (except for the transient effect on T cells) or depletion of BM HSC populations. Finally, as shown in Figure S2A (bottom row), CY treatment at a dose of 125 mg/kg was both necessary and sufficient pre-treatment to achieve the goal of $CXCR4^+$ c-kit CAR-T cell-mediated depletion of the KSL population in BM. Furthermore, the importance of CY pre-treatment to achieve the $CXCR4^+$ c-kit CAR-T cell-mediated depletion of KSL from the BM was demonstrated by the studies shown in Figure S2B, where increasing doses or 3 consecutive days of administrations of high doses of $CXCR4^+$ c-kit CAR-T cells without CY pre-treatment only modestly increased the percentage of these CAR-T cells in the BM at day 8 (Figure S2B, upper panel), and they did not deplete BM

**Figure 4. *In Vivo* Depletion of BM Cells after CY Only or after CY + $CXCR4^+$ c-kit CAR-T Cell Treatment**

(A) Time course of PB hemoglobin (Hgb), platelets (Plt), total leukocyte (WBC), and absolute neutrophil (Neut) count following CY alone (blue), CY + $CXCR4^-$ c-kit CAR-T (orange), or CY + $CXCR4^+$ c-kit CAR-T cell (red) compared with the naive (purple) (n = 5; mean ± SD; ***$p < 0.001$, **$p < 0.01$, and *$p < 0.05$). (B) Photomicrographs of H&E-stained tibia sections from naive mouse or mice following CY only, CY + $CXCR4^-$ c-kit CAR-T, or CY + $CXCR4^+$ c-kit CAR-T cell injection. (C) Photographs of *in vitro* colony formation assay of BM cells from naive mice or mice on day 12 following CY only, CY + $CXCR4^-$ c-kit CAR-T, or CY + $CXCR4^+$ c-kit CAR-T cell injection. Numbers of colonies per plate are shown in the graph (n = 5; mean ± SD; ***$p < 0.001$; NS, not significant). (D) FACS analysis of BM obtained from naive mice or from mice at days 4 and 8 after treatment with CY only, CY + $CXCR4^-$ c-kit CAR-T, or CY + $CXCR4^+$ c-kit CAR-T cells, where boxes show percentage of KSL ($c\text{-}kit^+sca1^+Lineage^-$) cells. (E) Time course of the same FACS analyses of mice as indicated in (D), but calculating and plotting absolute number of BM, $c\text{-}kit^+$, KSL, or LT-HSC cells per 2 femurs per mouse (n = 3 [5 mice/experiment; 15 mice total]; mean ± SD; ***$p < 0.001$, **$p < 0.01$, and *$p < 0.05$).

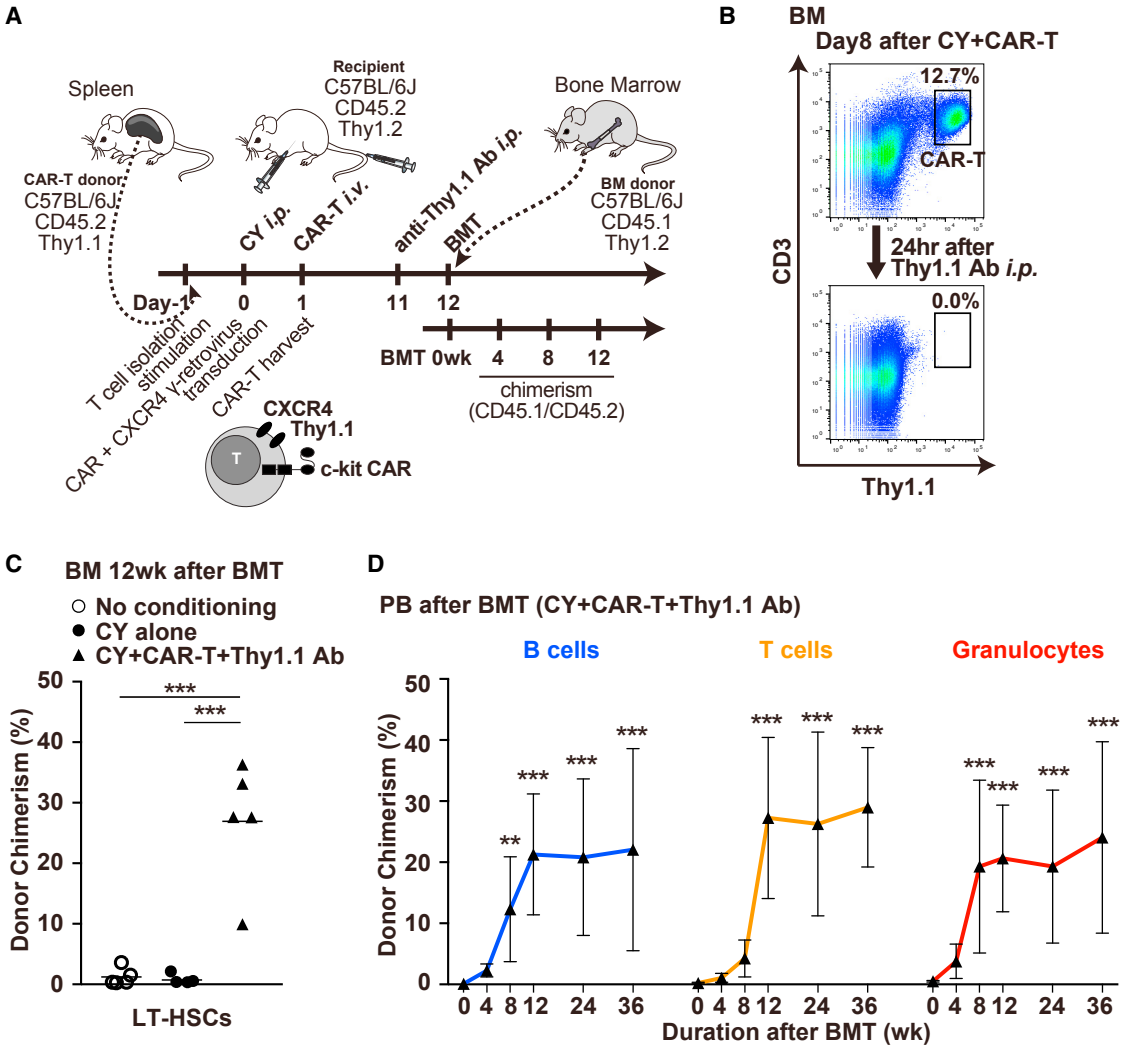


**Figure 5. CY Plus Congenic Thy1.1$^+$ CD45.2$^+$ CXCR4$^+$ c-kit CAR-T Cell Facilitated Engraftment of Congenic Donor Thy1.2$^+$ CD45.1$^+$ BM into Thy1.2$^+$ CD45.2$^+$ C57BL/6J Mice following the Depletion of CAR-T Cells with Anti-Thy1.1 Antibody**

(A) Timeline of c-kit CAR-T cell production and *in vivo* injection followed by Thy1.1 antibody depletion of c-kit CAR-T cells, transplantation of donor BM, and subsequent evaluation of donor engraftment. (B) FACS analysis of congenic Thy1.1$^+$ CD45.2$^+$ CXCR4$^+$ c-kit CAR-T cells in recipient BM at day 8 comparing before and 24 hr after (day 9) i.p. injection of anti-Thy1.1 antibody (upper versus lower panels). (C) Percentage of all LT-HSCs in recipient BM that are donor phenotype by FACS analysis at 12 weeks after transplant without conditioning, with CY alone, or after CY plus c-kit CAR-T cell conditioning and Thy1.1 antibody depletion of the c-kit CAR-T cells (n = 5; mean ± SD; ***p < 0.001). (D) Time course of percentage of B cell, T cell, and granulocyte lineages in the PB that are donor phenotype by FACS analysis at 0, 4, 8, and 12 weeks and 6 and 9 months after transplant mediated by CY plus c-kit CAR-T cell conditioning and Thy1.1 antibody depletion of the c-kit CAR-T cells (n = 3 [5 mice/experiment; 15 mice total]; mean ± SD; ***p < 0.001 and **p < 0.01).

KSL cells (Figure S2B, lower panel). In fact, at highest doses of CXCR4$^+$ c-kit CAR-T cells without CY pre-treatment, there was an unexplained increase in KSL cells.

### BM Transplantation for Mice Treated with c-kit CAR-T Cells

Having confirmed that CY conditioning plus CXCR4$^+$ c-kit CAR-T cell treatment is highly effective in depleting BM HSCs, we next determined procedures that would deplete the CXCR4$^+$ c-kit CAR-T cells sufficiently to allow subsequent engraftment of donor BM. Although in the future it should be possible to add suicide elements to the CAR-T cell construction to allow elimination of these cells once BM HSC had been sufficiently depleted, for our current mouse model system we were able to use specific anti-Thy1.1 antibodies to achieve effective *in vivo* depletion of the congenic Thy1.1$^+$ CXCR4$^+$ c-kit CAR-T cells from Thy1.2-recipient mice. As indicated in the timeline shown in Figure 5A, by using congenic Thy1.1$^+$ CD45.2$^+$ CXCR4$^+$ c-kit CAR-T cells to treat Thy1.2$^+$ CD45.2$^+$ C57BL/6J mice, and using congenic Thy1.2$^+$ CD45.1$^+$ BM as donor cells, it was possible to use anti-Thy1.1 antibody to deplete the Thy1.1$^+$ CD45.2$^+$ CXCR4$^+$ c-kit CAR-T cells *in vivo* before donor BM transplant, and then to be able to follow

Thy1.2$^+$ CD45.1$^+$ donor BM engraftment in the Thy1.2$^+$ CD45.2$^+$ host. In this scheme, production of Thy1.1$^+$ CD45.2$^+$ CXCR4$^+$ c-kit CAR-T cells, CY pre-treatment (125 mg/kg), and injection of these c-kit CAR-T cells were performed per the methods and timetable in experiments in Figures 3 and 4, except that at day 11 mice were injected i.p. with anti-Thy1.1 antibody and transplanted with donor BM on day 12 (Figure 5A). When discussing donor chimerism assessed post-transplant, the day of BM transplant is re-set as day 0/Week 0. We demonstrate that Thy1.1$^+$ CD45.2$^+$ CXCR4$^+$ c-kit CAR-T cells were completely depleted from the Thy1.2$^+$ CD45.2$^+$ C57BL/6J recipient mice at 24 hr after a single i.p. injection with 500 μg anti-Thy1.1 antibody (Figure 5B, compare top and bottom panels). Also following anti-Thy1.1 antibody treatment, there were no residual c-kit CAR-T cells detected in PB, spleen, thymus, and lymph nodes as assessed by FACS analysis (Figure S4). At 24 hr after Thy1.1 antibody treatment, recipient mice were injected by tail vein with $3 \times 10^6$ BM cells from Thy1.2$^+$CD45.1$^+$ donor mice that had been prepared for donation by 5-fluorouracil (150 mg/kg, 4 days before harvest).

As shown in Figures 5C and 5D, congenic donor BM was transplanted into recipient mice that received neither CY nor CXCR4$^+$ c-kit CAR-T cells (no conditioning); into recipient mice receiving CY, but not CXCR4$^+$ c-kit CAR-T cells (CY alone); or into recipient mice that received CY pre-treatment plus CXCR4$^+$ c-kit CAR-T cells and subsequent depletion with Thy1.1 antibody (CY + CAR-T + Thy1.1 Ab). PB was sampled at 4-week intervals. The mice from one of the three experiments (5 mice per condition) were sacrificed at 12 weeks to assess BM engraftment by determining the percentage of LT-HSCs that were donor phenotype (CD45.1$^+$ CD45.2$^-$), while mice from the other two experiments were kept alive so that PB could continue to be sampled for a much longer period of time. At 12 weeks, there was essentially no donor engraftment of LT-HSCs in mice receiving no conditioning or with CY alone, but engraftment of the donor LT-HSC phenotype in mice receiving the CY + CAR-T + Thy1.1 Ab-conditioning regimen ranged from 9.9% to 36.3% with a mean of 26.9% (Figure 5C). PB was sampled at 4-week intervals from all mice in the three experiments (5 mice per experiment per condition). There was no detectable engraftment of donor lineages in the PB of transplanted mice receiving either no conditioning or CY alone treatment (data not shown). In Figure 5D is shown the time course of appearance of donor cells in 3 lineages of the PB assessed up to 9 months in all 15 transplanted recipient mice who had received the CY + CAR-T + Thy1.1 Ab-conditioning regimen. Donor chimerism for granulocytes plateaued at 8 weeks, where at 8 and 12 weeks chimerism averaged 22.9% (range ~11%–36%). As would be expected, there was a lag in PB donor B and T cell chimerism, but by 12 weeks it was similar to that of PB granulocytes. Residual CAR-T cells were not detected in the PB at any time points after transplantation by FACS analyses.

### Treatment of CGD Mice Using c-kit CAR-T Cell Conditioning and BM Transplantation

We next applied c-kit CAR-T cell conditioning to wild-type donor mouse BM transplant of the X-linked chronic granulomatous disease (CGD) mouse, as shown in Figure 6A. This CGD mouse has a disruptive insertion in the gene encoding the gp91-phox subunit of the phagocyte NADPH oxidase, such that granulocytes and monocytes fail to produce microbicidal reactive oxygen species (ROS) when stimulated.[30] The functional defect in ROS generation can be measured in PB granulocytes using the dihydrorhodamine 123 (DHR) flow cytometry assay,[31] as shown in Figure 6B, where phorbol 12-myristate 13-acetate (PMA) stimulation of normal results in ROS mediated conversion of DHR to highly fluorescent rhodamine in >98% of normal wild-type mouse granulocytes (Figure 6B, middle panel), which is lacking in stimulated CGD mouse granulocytes (Figure 6B, right panel). In the CGD mice, the BM KSL population was almost the same as normal C57BL/6J mice (Figure 6C, left panel), and this population was completely depleted after the treatment with CY + CAR-T and BM displayed severe aplasia, just as we observed in the normal C57BL/6J mice (Figure 6C, right panel). After c-kit CAR-T cell mediated transplantation of BM from naive mice (Thy1.2$^+$CD45.1$^+$) to CGD mice (Thy1.2$^+$CD45.2$^+$) following the scheme in Figure 6A, there was now normal production of ROS from the engrafted CD45.1$^+$ donor granulocytes (Figure 6D, middle panel). In the mouse analyzed in this panel, 35% of circulating granulocytes were DHR positive. The time course shown for reconstitution of oxidase normal granulocytes in the PB of 5 CGD mice transplanted with normal wild-type BM following c-kit CAR-T cell conditioning is shown in Figure 6D (right panel). At week 12 the average percentage of oxidase-normal granulocytes in the PB of these transplanted CGD mice was 28% (range 18%–36%).

## DISCUSSION

In the current study, we have established a mouse c-kit CAR-T cell BM-conditioning method to achieve substantial engraftment of congenic donor BM. In our *in vitro* and *in vivo* studies, we specifically show that (1) mouse c-kit CAR-T cells *in vitro* specifically bind and kill c-kit$^+$ cells (including both cell lines and BM cells), and this killing is associated with high-level IFNγ release by the c-kit CAR-T cells; (2) mouse c-kit CAR-T cells require transduction-mediated overexpression of CXCR4 to achieve adequate migration into the BM; (3) pre-treatment of mice with low-dose CY (125 mg/kg) 1 day prior to the administration of CXCR4$^+$ c-kit CAR-T cells is both necessary and sufficient to achieve the required expansion of c-kit CAR-T cells that is needed to significantly deplete LT-HSCs or KSL cells from recipient BM; (4) this expansion and increased migration into the BM by the CXCR4$^+$ c-kit CAR-T cells resulted in persistent BM aplasia and eventual death from aplastic anemia; and, (5) following the achievement of BM depletion over 10 days, elimination of the CXCR4$^+$ c-kit CAR-T cells can be accomplished using Thy1.1 antibody to allow engraftment donor BM. These maneuvers, such as the initial CY administration, injection of CXCR4$^+$ c-kit CAR-T cells, followed by elimination of the CXCR4$^+$ c-kit CAR-T cells at a time of maximum recipient HSC depletion, allow >20% long-term congenic BM multilineage engraftment. An important aspect of the use of a CXCR4$^+$ c-kit CAR-T cell approach to BM conditioning is the avoidance of ionizing radiation or strong alkylating agents such as busulfan, which may also

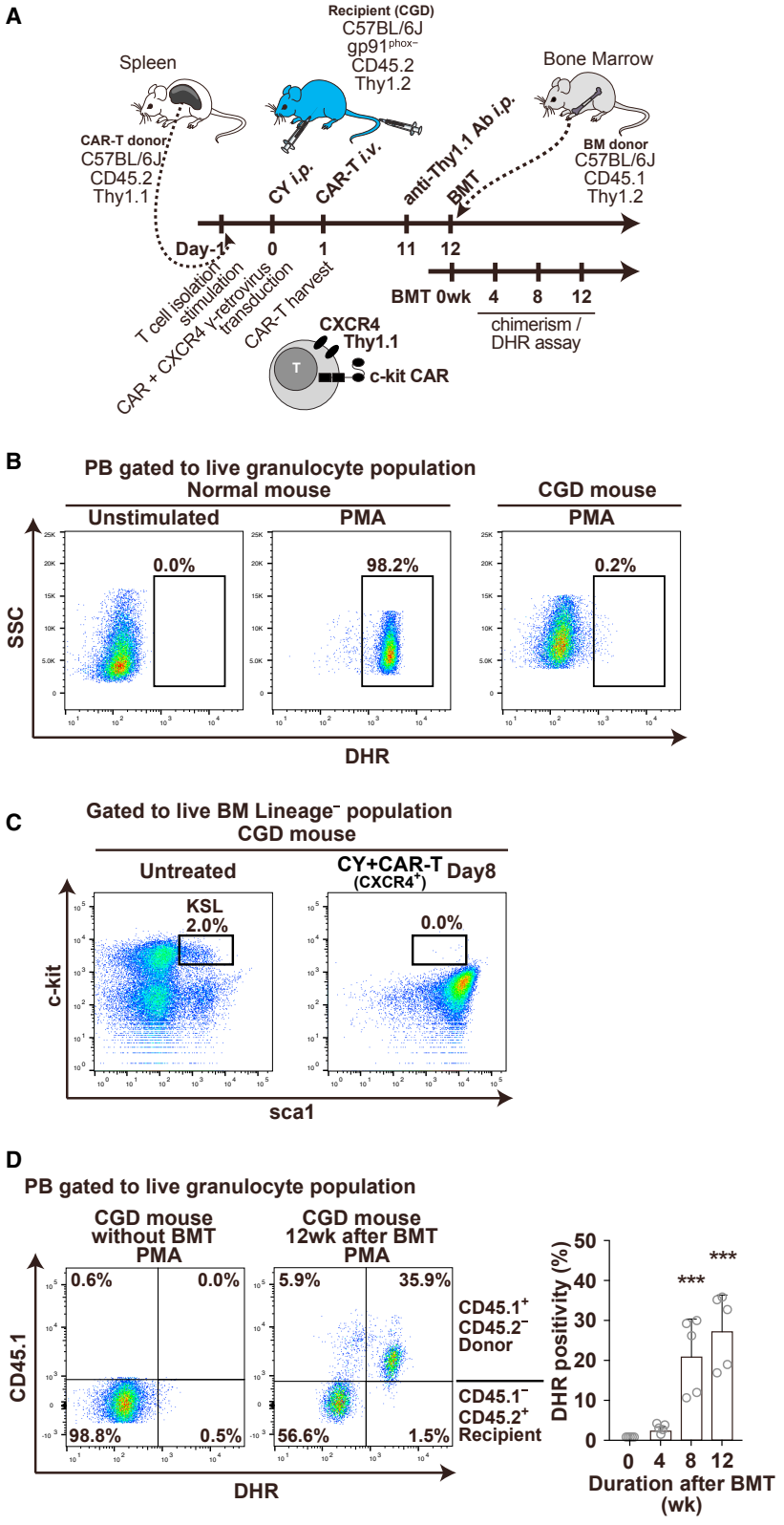


**Figure 6. Treatment of gp91-phox-Deficient CGD Mice with Normal Wild-Type BM Transplantation Using Sequential CY + CAR-T + Thy1.1 Ab Conditioning**

(A) Timeline of c-kit CAR-T cell production and *in vivo* injection into CGD mice followed by Thy1.1 antibody depletion of c-kit CAR-T cells, transplantation of donor normal wild-type BM, and subsequent evaluation of donor engraftment and assessment of the appearance of $DHR^+$ oxidase normal granulocyte in the PB of transplanted CGD mice. (B) DHR flow cytometry analysis of ROS production by PB granulocytes without or with PMA stimulation from a normal wild-type mouse (middle and left panels) or CGD mouse (right panel) (gated on granulocyte $Gr1^+Mac1^+$ population). (C) FACS analysis of BM obtained from untreated and CY + CAR-T-treated CGD mice at day 8, where boxes show percentage of KSL ($c\text{-}kit^+sca1^+Lineage^-$) cells. (D) Normal wild-type donor PB granulocyte chimerism (CD45.1) in c-kit CAR-T cell-conditioned CGD mice (CD45.2) was assessed together with measurement of DHR oxidase activity (PMA stimulation) before transplantation (left panel) and 12 weeks after transplantation of normal wild-type BM into CGD mice conditioned with c-kit CAR-T cells (right panel). Time course of percentage of $DHR^+$ cells (in granulocyte fraction) is shown in right panel at 0, 4, 8, and 12 weeks after transplantation (n = 5; mean ± SD; ***$p < 0.001$).

damage or inflame both BM and thymus stroma, and this may provide a more favorable environment for BM transplant and restoration of lymphoid immunity.[32]

The γ-retrovirus c-kit CAR construct, which we used in this study to produce mouse c-kit CAR-T cells, showed high efficacy of transduction, and the resultant c-kit CAR-T cells demonstrated high specificity and robust cytotoxicity, activity of which depends on the extracellular single-chain variable fragment (scFv) and the intracellular signaling domain. Many studies have examined the effect of various arrangements of extracellular scFv domains for CAR-T cells, assessing the effect on functional activity of the orientation of $V_L$ and $V_H$ and the types of linker domain between these variable regions in the constructs.[25,33] To date, there are no strategies that can predict the most suitable structure for each individual CAR construct without empiric assessment. To achieve optimum design of our final c-kit CAR, we produced c-kit CAR-T cells with multiple combinations of scFv (Figure S1), and we found that only one of the combinations we constructed and assessed could efficiently generate highly functional CAR-T cells targeting c-kit$^+$ cells for efficient killing.

Given the highly effective killing of c-kit$^+$ cell lines or primary BM HSCs in culture by our c-kit CAR-T cells, we were disappointed to find that simply injecting even very large numbers of these cells into mice without other maneuvers resulted in no depletion of BM HSCs *in vivo*. We did not present in the Results our initial alternative attempts to improve the effect of the c-kit CAR-T cells that included pre-treatment with low-dose busulfan and/or low-dose radiation, neither of which achieved any synergy with the c-kit CAR-T cells in killing BM HSCs *in vivo*. We also failed to observe any HSC depletion when we tried using plerixafor (CXCR4 antagonist) to mobilize HSCs into the PB, hoping that would increase access of the c-kit CAR-T cells to HSCs. The next strategy we tried was administration of CY, based on the observation from human clinical trials using CAR-T cells,[20,21] where pre-treatment with a T cell-depleting agent such as CY significantly enhanced efficacy in part by stimulating expansion *in vivo*. In that setting CY might also be working to eliminate endogenous regulatory T cells.[34] The use of CY in our mouse model achieved significant expansion of the c-kit CAR-T cells *in vivo*, including increased numbers in the BM, and it did result in a slow pace of depletion of BM cells, but still it was not itself sufficient to observe the rapid complete elimination of LT-HSC phenotype cells. We previously demonstrated that transduction-forced overexpression of CXCR4 in HSCs can increase engraftment in BM, even though HSCs naturally express endogenous CXCR4.[28] Similarly, T cells express some endogenous CXCR4, but we postulated that transduction-forced higher expression of CXCR4 on the c-kit CAR-T cells might not only increase the efficiency and speed of trafficking to BM but also might increase retention within the BM as well as bringing them into more intimate contact with HSCs. This final maneuver (CXCR4 overexpression) together with low-dose CY pre-treatment achieved the required goal of highly efficient rapid clearance by day 8 of c-kit$^+$ cells from the BM, particularly those with LT-HSC markers.

Regarding the choice of CY dosage, we were guided by previous studies of the use of CAR-T cells for tumor killing in mouse models where CY at 100–250 mg/kg had been explored and shown to be effective.[26,27] To the best of our knowledge, it had not been possible to observe efficient tumor targeting-effects from second-generation CAR-T cells in immunocompetent mice without the use of CY or other lymphocyte depletion strategies. The function and effect of low-dose CY *in vivo*, which mainly relies on its metabolites (particularly 4-hydroxy-cyclophosphamide),[35] have been seen to depend on both overall suppression of lymphocytes and effects on regulatory T cells.[36] Moreover, higher doses of CY than we used in our study or the combination of other chemotherapies were necessary to induce HSC depletion in BM and to allow donor graft to be engrafted in the immunocompetent mice; 400 mg/kg CY,[37] 40–70 mg/kg busulfan plus 200 mg/kg CY,[38–40] or 300 mg/kg fludarabine and 150 mg/kg CY[41] were used as BM-conditioning protocols in previous studies. In our study, we selected 125 mg/kg i.p., which was the minimal dose we found empirically to be required for CAR-T cell expansion and to achieve the desired effect of the c-kit CAR-T cells on BM HSCs, but which did not itself without c-kit CAR-T cells have any effect on BM cellularity, BM colony formation, or PB cell counts. Not shown is that we measured and confirmed that regulatory T cells were depleted by low-dose CY (125 mg/kg), an effect that might be in part responsible for the expansion, migration into BM, and enhanced killing of BM HSCs by CXCR4$^+$ c-kit CAR-T cells.

CXCR4 is the chemokine receptor for C-X-C chemokine ligand (CXCL) 12, known as stromal cell-derived factor (SDF)-1α, which is broadly expressed in the BM HSC niche.[42] Expression of CXCR4 on the cell surface works both as a homing signal to BM and as a retention signal for cells in the BM. HSCs naturally express endogenous CXCR4,[42] but forced additional expression by transduction of CXCR4 enhances the engraftment of HSCs.[28] Moreover, gain-of-function mutations of CXCR4 are a cause of WHIM syndrome, which results in a panleukocytopenia in the PB but hyperplasia in the BM, including retention of neutrophils in the BM to their point of senescence, suggesting that this stronger binding with WHIM mutant C-terminal-truncated CXCR4 prevents the release of neutrophils into the PB from the BM.[29] From this, it is possible to postulate that transduction-mediated increased CXCR4 expression in the c-kit CAR-T cells not only enhances migration but also increases retention in the BM. A previous study in human HSCs indicated that CD34$^+$ cells express both CXCR4 and CXCR4 ligand (CXCL12),[43] raising the possibility that the co-expression of CXCR4 on the CAR-T cells might be serving as a bi-functional binding element with the c-kit-binding element in targeting mouse HSC. However, cell surface expression of CXCL12 was not detected in whole BM and the KSL population in our mouse study (Figure S5). Because CXCL12 is particularly highly expressed in the BM niche on stromal cells,[42] overexpression of CXCR4 could reduce off-target effects of c-kit CAR-T cells. However, there is expression of c-kit by tissues outside of the BM, including germ cells, melanocytes, Cajal cells of the gastrointestinal tract, and subsets of cerebellar neurons in addition to BM HSCs/progenitor cells.[44] Despite this, we did not

grossly observe off-target effects such as hair graying from any effect on melanocytes, which was reportedly observed after anti-mouse c-kit antibody (ACK2) administration.[45]

As noted, the transduction-mediated overexpression of CXCR4 in the c-kit CAR-T cells had a major impact on the pace and extent of clearance of HSCs from the BM. This successful use of a chemokine receptor to direct and possibly hold CAR-T cells to a desired anatomic location, where their action on a target cell type may be amplified, may be one of the most important findings of our studies in that it may provide a general principle that could be applied to other applications of CAR-T cells. Specific to CXCR4-mediated targeting, it is possible that its use for CAR-T cells directed at antigens to treat myeloid leukemia might augment effectiveness in the way that its use in our study augmented the effectiveness of c-kit CAR-T cell killing of HSCs in the BM. Solid tumors or myeloid leukemia has proven to be a particularly difficult target for CAR-T cell treatments, likely for a variety of reasons,[46] but it is possible that influencing trafficking to and/or tethering in a solid tumor by increased expression of a migration or tethering receptor might be a useful element to explore.[47]

In conclusion, our findings in this mouse study provide a first proof of concept that $CXCR4^+$ c-kit CAR-T cells can be used to achieve BM HSC clearance sufficient to result in substantial (>20%) levels of long-term stable multilineage engraftment of congenic BM in immunocompetent mice. Despite this accomplishment, more work is required to optimize this approach to achieve higher levels of engraftment in both the congenic setting and in a partial major histocompatibility complex (MHC) mismatch setting that we did not explore in this study. In addition, there are applicability and safety issues that must be addressed before being able to consider this for a human treatment setting. For example, in the congenic mouse models we used for this study, anti-Thy1.1 antibody proved highly effective at completely eliminating the $Thy1.1^+CXCR4^+$ c-kit CAR-T cells in the $Thy1.2^+$ recipient to allow engraftment of congenic BM, but, in the future, we will need to explore alternate strategies more applicable to the human setting to eliminate the $CXCR4^+$ c-kit CAR-T cells such as the built-in suicide gene system,[48] mRNA-electroporated CAR-T cells, T cell ablation with alemtuzumab, or CAR-T cell ablation with rituximab by using CD20-coexpressing CAR-T cells.[49] Other maneuvers that we will explore that might further enhance the efficiency of the c-kit CAR-T cells might include use of C-terminal-truncated versions of CXCR4 that imitate WHIM syndrome mutations that greatly enhance the activity of this receptor by interfering with internalization and downregulation.

## MATERIALS AND METHODS

### Construction of γ-Retrovirus Encoding c-kit CAR and Transduction of Mouse T Cells

We determined the cDNA sequence of the ACK2 monoclonal anti-mouse c-kit antibody by extracting mRNA from the hybridoma cell line.[50] Reverse-transcribed cDNA was subject to rapid amplification of cDNA ends (RACE) PCR (SMARTer RACE 5′/3′ Kit, Clontech Laboratories, Mountain View, CA, USA) using the universal primer for variable regions of immunoglobulin heavy and light chains ($V_H$ and $V_L$).[51] The PCR products generated were inserted into a cloning vector (Zero Blunt TOPO PCR cloning kit, Invitrogen, Carlsbad, CA, USA), and DNA sequence was determined using Sanger method by Macrogen USA (Rockville, MD, USA). From the obtained sequence information, variable regions in both chains were determined using an online database program (IMGT/V-QUEST program, version 3.4.7). Double-stranded DNA including these two regions ($V_H$ and $V_L$) was connected with either of two linker sequences previously employed in CAR construction (the 218 linker[33] or the $(G_4S)_3$ linker[25]) and followed by the downstream mouse CD8, CD28, and CD3ζ cDNA[52] that had been synthesized *in vitro* (Integrated DNA Technologies, Coralville, IA, USA); and it was cloned into retroviral vector backbone containing the MSGV promotor.[52]

This retroviral vector plasmid (pMSGV c-kit CAR) was transfected into the Platinum-E, a 293T-based retroviral packaging cell line with ecotropic envelope (plat-E) (Cell Biolabs, San Diego, CA, USA). Transfection of confluent plat-E was performed in 10-cm dish using 12 μg pMSGV c-kit CAR plasmid along with transfection reagent (15 μL X-treamGENE HP DNA Transfection Reagent, Roche Applied Science, Mannheim, Germany), and γ-retrovirus was harvested 48 and 72 hr later. As a control, previously described γ-retrovirus-encoding mouse VEGFR-2 CAR[24] was prepared in the same way.

As donors of T cells, C57BL/6J mice congenic for Thy1.1 (wild-type C57BL/6J strain are Thy1.2) were purchased (B6.PL-*Thy1*$^a$/CyJ, JAX406, The Jackson Laboratory, Bar Harbor, ME, USA). Spleens were harvested from this strain (8–12 weeks old), and T cells were isolated from them using negative selection technique (Dynabeads Untouched Mouse T Cells, Invitrogen), followed by *in vitro* culture with CD3/28 antibody stimulation (Dynabeads Mouse T-Activator CD3/CD28, Gibco, Gaithersburg, MD, USA). For the purpose of transduction, γ-retrovirus for c-kit CAR (or VEGFR-2 CAR as the control) was adhered to the fibronectin-coated culture plate (RetroNectin, Takara Bio, Shiga, Japan) (centrifuging at 2,500 rpm for 2 hr); then, stimulated and expanded T cells were infected with γ-retrovirus on the plate. CAR expression was evaluated by FACS (FACS Canto, BD Biosciences, San Jose, CA, USA) at 24–48 hr after transduction with the staining of mouse anti-Fab antibody conjugated with biotin (Jackson ImmunoResearch Laboratories, West Grove, PA, USA) and imaged with streptavidin PE (BD Biosciences). Recombinant mouse c-kit protein conjugated with mouse Fc or mouse VEGFR-2 protein conjugated with human Fc (c-kit-Fc and VEGFR-2-Fc obtained from R&D Systems, Minneapolis, MD, USA) along with anti-mouse/human Fc-APC secondary antibodies (Jackson ImmunoResearch) was used to evaluate the specific binding of CAR-T cells to the target proteins. For all FACS studies noted here or below, cells were stained with Zombie NIR Fixable Viability Kit (BioLegend, San Diego, CA, USA) to allow gating to distinguish alive and dead cells.

We also constructed a γ-retrovirus vector plasmid encoding cDNA for mouse CXCR4 (plasmid encoding murine CXCR4 from OriGene,

Rockville, MD, USA), and we prepared ecotropic enveloped vector as outline above using plat-E. For those experiments requiring c-kit CAR-T cells also expressing excess CXCR4, T cells were co-transduced with both the c-kit CAR vector and the CXCR4 vector in the same culture. Surface expression of CXCR4 was detected with anti-mouse CXCR4 antibody (BD Biosciences).

### *In Vitro* Co-culture Assay

Mouse cell lines with strong expression of c-kit were prepared to use as targets of c-kit CAR-T cells. NIH 3T3 (originally sourced from American Type Culture Collection, Manassas, VA, USA) and the mouse B cell leukemia cell line that expressed CD19 (E2a-PBX)[53] were each transduced for three times with a third-generation lentivirus[54] into which we substituted mouse c-kit cDNA sequence (OriGene). Cell surface c-kit expression was confirmed by FACS after staining with anti-mouse c-kit antibody (BD Biosciences). To enhance visibility under the fluorescent microscope, the NIH 3T3 cells in some experiments were co-transduced with the same lentivector encoding GFP.

For the *in vitro* co-culture assay of target cell killing by CAR-T cells, the various c-kit-expressing and control target cell lines ($2.5 \times 10^5$ cells) and mouse unfractionated BM (harvested from wild-type C57BL/6J with CD45.2$^+$Thy1.2$^+$; JAX664 purchased from The Jackson Laboratory) were mixed with CAR-T cells and controls ($4.0 \times 10^3$–$2.5 \times 10^5$ cells from CD45.2$^+$Thy1.1$^+$ mice) in the 24-well plate for 24 hr. Harvested supernatant was subjected to ELISA assay of mouse IFNγ (Quantikine ELISA, R&D Systems), and cultured cells were analyzed with FACS using anti-mouse CD19, CD3, and c-kit antibodies (BD Biosciences). NIH 3T3 cells (marked with GFP) were examined and photographed by fluorescent microscopy analyses (EVOS FL Cell Imaging System, Life Technologies, Carlsbad, CA, USA) to determine the viability after one-time gentle wash following 24-hr co-culture.

BM cells ($4 \times 10^4$ cells) co-cultured with c-kit CAR-T cells were transferred to nitrocellulose medium with complete cytokines in a 6-cm dish (Methocult medium, STEMCELL Technologies, Vancouver, Canada) after 24-hr incubation in the normal RPMI-1640 medium (Life Technologies). Colony number was counted visually or photographed on day 10 using an inverted microscope (Eclipse T*i*-U, Nikon Instruments, Melville, NY, USA), with colony type enumerated according to each type of colony (BFU-E, CFU-M, -G, -MG, and -GEMM), though for most studies the total number of colonies was compared among each condition.

### *In Vivo* Injection of CAR-T Cells and Evaluation of Their Function

CAR-T cells generated from the abovementioned donor mice spleen T cells (C57BL/6J with CD45.2$^+$Thy1.1$^+$) or from luciferase-transgenic mice (B6;FVB-*Ptprc*$^a$ Tg(CAG-luc,-GFP)L2G85Chco *Thy1*$^a$/J; JAX25854 purchased from the Jackson Laboratory) were harvested 24 hr after γ-retrovirus transduction and re-suspended in the infusion buffer (PBS with 0.1% BSA) (Sigma-Aldrich, St. Louis, MO, USA) at the concentration of $5 \times 10^6$ cells/100 μL. Recipient mice (C57BL/6J with CD45.2$^+$Thy1.2$^+$) without or with administration of low-dose CY i.p. (125 mg/kg) (Sigma-Aldrich) were subjected to CAR-T cell injection intravenously via tail vein 24 hr after CY treatment. For some experiments, different dosing of CY (62.5 mg/kg, 125 mg/kg, and 250 mg/kg) was explored.

Expansion and trafficking of injected CAR-T cells (generated from luciferase transgenic mice described above) were analyzed by an *in vivo* imaging system (In-Vivo Xtreme, Bruker, Billerica, MA, USA). Luciferase-transgenic mice c-kit CAR-T cells (without or with co-transduction of CXCR4) were injected into recipient mice, and 7 days after injection they were treated with luciferin i.p. injection (3 mg) (VivoGlo Luciferin, Promega, Madison, WI, USA), and emitted whole-body fluorescence was detected by *in vivo* imaging. The pictures were overlaid onto the X-ray images of each mouse to determine the anatomic correlations.

CAR-T cell presence and effects *in vivo* were assessed by PB count and BM harvest count, as well as FACS assessment of lineages. BM populations were also analyzed by colony formation assay and histology. PB cell counts were determined with automated hemocytometer (Hemavet 950, Drew Scientific Group, Miami Lakes, FL, USA), and BM cell numbers per two femurs were calculated in each mouse using trypan blue staining to assess live cells (Lonza, Walkersville, MD, USA). For FACS analysis, cells were stained with anti-mouse Thy1.1, Thy1.2, CD3, CD19, c-kit, sca1, CD135, and CD34 antibodies along with the lineage mix cocktail (BD Biosciences), and they were analyzed with FACS Canto or Fortessa (BD Biosciences). For colony assay, BM cells ($4 \times 10^4$ cells) harvested from the treated mice were transferred to Methocult nitrocellulose medium with complete cytokines, and colony number was counted on day 10. In some experiments, H&E-stained slides of tibia were prepared by American Histolabs (Gaithersburg, MD, USA) and analyzed to determine the cellularity of BM using the microscopy (Axio ImagerZ1, Carl Zeiss Vision, San Diego, CA, USA).

### BM Transplant after CAR-T Cell Injection and Chimerism Evaluation

Recipient mice (C57BL/6J with CD45.2$^+$Thy1.2$^+$) injected with CXCR4$^+$ c-kit CAR-T cells (derived from C57BL/6J with CD45.2$^+$ Thy1.1$^+$ mice) after low-dose treatment of CY (125 mg/kg i.p.) were injected with 500 μg anti-mouse Thy1.1 antibody by i.p. administration (*InVivo*mAb anti-mouse Thy1.1, clone 19E12, Bio X Cell, West Lebanon, NH, USA) on day 11 in order to deplete CAR-T cells. These recipient mice were then transplanted with BM cells harvested from C57BL/6J with CD45.1$^+$Thy1.2$^+$ donor mice (B6.SJL-*Ptprc*$^a$ *Pepc*$^b$/BoyJ; JAX2014 purchased from The Jackson Laboratory). The BM donor mice were pre-treated with 150 mg/kg 5-fluorouracil (Sigma-Aldrich) 4 days before BM harvest to deplete mature cells,[55] and $3 \times 10^6$ donor BM cells per recipient mouse were intravenously transplanted by tail vein.

Chimerism between CD45.1 (donor) and CD45.2 (recipient) cells was determined at 4, 8, and 12 weeks and 6 and 9 months in the PB, and

some mice were sacrificed at 12 weeks to harvest and examine lineages in the BM, including KSL or c-kit$^+$ HSCs. Anti-mouse CD45.1 and CD45.2 antibodies were used along with T cell (CD3$^+$), B cell (CD19$^+$), granulocyte (Gr-1$^+$Mac1$^+$), and long-term HSC (LT-HSC; Lineage$^-$c-kit$^+$sca1$^+$CD135$^-$CD34$^-$) markers to perform FACS analyses for the chimerism assessment (BD Biosciences).

For CGD mouse treatment experiments, gp91-phox-deficient mice (B6.129S-*Cybb*$^{tm1Din}$/J; JAX2365 purchased from the Jackson Laboratory) were used as recipients (Thy1.2$^+$CD45.2$^+$), and they were transplanted with BM from C57BL/6J CD45.1$^+$Thy1.2$^+$ donor normal wild-type mice using the same conditioning protocol that sequentially employs CY + CAR-T + Thy1.1 Ab. For the post-transplant analysis of ROS, production by PB granulocytes was measured using the DHR assay.[31] More specifically, mouse PB was subjected to erythrocyte lysis and loading of DHR (LifeTechnologies) followed by stimulation with PMA (final 10 ng/μL) for 15 min. ROS production by DHR analysis was detected in the granulocyte (Gr-1$^+$Mac1$^+$) fraction.

All the animal studies were in accordance with NIH Guide for the Care and Use of Laboratory Animals, and the specific experiments and mouse strains were approved by the National Institute of Allergy and Infectious Disease Animal Care and Use Committee (NIAID ACUC) under animal use protocol LHD-3E (now LCIM-1E).

### Statistical Analyses

Experiments were repeated at least 3–5 times independently, though some transplant studies where specifically indicted were a single experiment with 5 mice. Values were described as the mean ± SDs. Data were compared with Student's t test or ANOVA, and statistical analyses were performed using GraphPad Prism (version 7.0c, GraphPad, La Jolla, CA). The alpha level of all tests or the p value was set at 0.05.

## SUPPLEMENTAL INFORMATION

Supplemental Information includes five figures and can be found with this article online at https://doi.org/10.1016/j.ymthe.2018.03.003.

## AUTHOR CONTRIBUTIONS

Y.A. and H.L.M. initiated the concept and designed the study. Y.A., C.I.C., and S.M.K. performed the experiments and collected the data. U.C., M.T., C.L.S., M.A.B., S.A.F., and M.C.D. provided critical materials and/or also provided critical advice and comments about methods and design during the conduct of this study. Y.A. and H.L.M. drafted the manuscript and all the authors edited and approved the final article.

## CONFLICTS OF INTEREST

The authors declare no conflict of interest.

## ACKNOWLEDGMENTS

The hybridoma cell line for mouse c-kit antibody (ACK2) was a gift from Dr. Shinichi Nishikawa, Dr. Satomi Nishikawa (All About Science Japan), and Dr. Minetaro Ogawa (Kumamoto University). The Mouse leukemia cell line (E2a-PBX) was obtained from Dr. Terry J. Fry (Pediatric Oncology Branch, National Cancer Institute). We also appreciate the help provided by Dr. Brenda Klaunberg (Mouse Imaging Facility, National Institute of Neurological Disorders and Stroke) for *in vivo* imaging and by Dr. Xingmin Feng (Hematology Branch, National Heart, Lung, and Blood Institute) for the PB cell counts in mice. This work was supported by the Intramural Program of NIAID, NIH within project Z01-AI-000988. Y.A. was recipient of a fellowship grant in support of this project from the Japan Society for the Promotion of Science (JSPS), Tokyo, Japan. M.C.D. obtained support from an award by the Children's Discovery Institute of Washington University and St. Louis Children's Hospital.

## REFERENCES

1. Kang, E.M., Marciano, B.E., DeRavin, S., Zarember, K.A., Holland, S.M., and Malech, H.L. (2011). Chronic granulomatous disease: overview and hematopoietic stem cell transplantation. J. Allergy Clin. Immunol. *127*, 1319–1326, quiz 1327–1328.

2. Heimall, J., Puck, J., Buckley, R., Fleisher, T.A., Gennery, A.R., Neven, B., Slatter, M., Haddad, E., Notarangelo, L.D., Baker, K.S., et al. (2017). Current Knowledge and Priorities for Future Research in Late Effects after Hematopoietic Stem Cell Transplantation (HCT) for Severe Combined Immunodeficiency Patients: A Consensus Statement from the Second Pediatric Blood and Marrow Transplant Consortium International Conference on Late Effects after Pediatric HCT. Biol. Blood Marrow Transplant. *23*, 379–387.

3. Srivastava, A., and Shaji, R.V. (2017). Cure for thalassemia major - from allogeneic hematopoietic stem cell transplantation to gene therapy. Haematologica *102*, 214–223.

4. De Ravin, S.S., Li, L., Wu, X., Choi, U., Allen, C., Koontz, S., Lee, J., Theobald-Whiting, N., Chu, J., Garofalo, M., et al. (2017). CRISPR-Cas9 gene repair of hematopoietic stem cells from patients with X-linked chronic granulomatous disease. Sci. Transl. Med. *9*, eaah3480.

5. Czechowicz, A., Kraft, D., Weissman, I.L., and Bhattacharya, D. (2007). Efficient transplantation via antibody-based clearance of hematopoietic stem cell niches. Science *318*, 1296–1299.

6. Xue, X., Pech, N.K., Shelley, W.C., Srour, E.F., Yoder, M.C., and Dinauer, M.C. (2010). Antibody targeting KIT as pretransplantation conditioning in immunocompetent mice. Blood *116*, 5419–5422.

7. Wulf, G.G., Luo, K.L., Goodell, M.A., and Brenner, M.K. (2003). Anti-CD45-mediated cytoreduction to facilitate allogeneic stem cell transplantation. Blood *101*, 2434–2439.

8. Chhabra, A., Ring, A.M., Weiskopf, K., Schnorr, P.J., Gordon, S., Le, A.C., Kwon, H.S., Ring, N.G., Volkmer, J., Ho, P.Y., et al. (2016). Hematopoietic stem cell transplantation in immunocompetent hosts without radiation or chemotherapy. Sci. Transl. Med. *8*, 351ra105.

9. Palchaudhuri, R., Saez, B., Hoggatt, J., Schajnovitz, A., Sykes, D.B., Tate, T.A., Czechowicz, A., Kfoury, Y., Ruchika, F., Rossi, D.J., et al. (2016). Non-genotoxic conditioning for hematopoietic stem cell transplantation using a hematopoietic-cell-specific internalizing immunotoxin. Nat. Biotechnol. *34*, 738–745.

10. Okada, S., Nakauchi, H., Nagayoshi, K., Nishikawa, S., Nishikawa, S., Miura, Y., and Suda, T. (1991). Enrichment and characterization of murine hematopoietic stem cells that express c-kit molecule. Blood *78*, 1706–1712.

11. Domen, J., and Weissman, I.L. (2000). Hematopoietic stem cells need two signals to prevent apoptosis; BCL-2 can provide one of these, Kitl/c-Kit signaling the other. J. Exp. Med. *192*, 1707–1718.

12. Kent, D., Copley, M., Benz, C., Dykstra, B., Bowie, M., and Eaves, C. (2008). Regulation of hematopoietic stem cells by the steel factor/KIT signaling pathway. Clin. Cancer Res. *14*, 1926–1930.

13. Dahlke, M.H., Larsen, S.R., Rasko, J.E., and Schlitt, H.J. (2004). The biology of CD45 and its use as a therapeutic target. Leuk. Lymphoma *45*, 229–236.

14. Hermiston, M.L., Xu, Z., and Weiss, A. (2003). CD45: a critical regulator of signaling thresholds in immune cells. Annu. Rev. Immunol. *21*, 107–137.

15. Chao, M.P., Majeti, R., and Weissman, I.L. (2011). Programmed cell removal: a new obstacle in the road to developing cancer. Nat. Rev. Cancer *12*, 58–67.

16. Bergamaschi, G., Perfetti, V., Tonon, L., Novella, A., Lucotti, C., Danova, M., Glennie, M.J., Merlini, G., and Cazzola, M. (1996). Saporin, a ribosome-inactivating protein used to prepare immunotoxins, induces cell death via apoptosis. Br. J. Haematol. *93*, 789–794.

17. Sadelain, M., Rivière, I., and Brentjens, R. (2003). Targeting tumours with genetically enhanced T lymphocytes. Nat. Rev. Cancer *3*, 35–45.

18. Eshhar, Z., Bach, N., Fitzer-Attas, C.J., Gross, G., Lustgarten, J., Waks, T., and Schindler, D.G. (1996). The T-body approach: potential for cancer immunotherapy. Springer Semin. Immunopathol. *18*, 199–209.

19. Rivière, I., and Sadelain, M. (2017). Chimeric Antigen Receptors: A Cell and Gene Therapy Perspective. Mol. Ther. *25*, 1117–1124.

20. Lee, D.W., Kochenderfer, J.N., Stetler-Stevenson, M., Cui, Y.K., Delbrook, C., Feldman, S.A., Fry, T.J., Orentas, R., Sabatino, M., Shah, N.N., et al. (2015). T cells expressing CD19 chimeric antigen receptors for acute lymphoblastic leukaemia in children and young adults: a phase 1 dose-escalation trial. Lancet *385*, 517–528.

21. Ali, S.A., Shi, V., Maric, I., Wang, M., Stroncek, D.F., Rose, J.J., Brudno, J.N., Stetler-Stevenson, M., Feldman, S.A., Hansen, B.G., et al. (2016). T cells expressing an anti-B-cell maturation antigen chimeric antigen receptor cause remissions of multiple myeloma. Blood *128*, 1688–1700.

22. Chang, Z.L., and Chen, Y.Y. (2017). CARs: Synthetic Immunoreceptors for Cancer Therapy and Beyond. Trends Mol. Med. *23*, 430–450.

23. Jacoby, E., Yang, Y., Qin, H., Chien, C.D., Kochenderfer, J.N., and Fry, T.J. (2016). Murine allogeneic CD19 CAR T cells harbor potent antileukemic activity but have the potential to mediate lethal GVHD. Blood *127*, 1361–1370.

24. Chinnasamy, D., Yu, Z., Theoret, M.R., Zhao, Y., Shrimali, R.K., Morgan, R.A., Feldman, S.A., Restifo, N.P., and Rosenberg, S.A. (2010). Gene therapy using genetically modified lymphocytes targeting VEGFR-2 inhibits the growth of vascularized syngenic tumors in mice. J. Clin. Invest. *120*, 3953–3968.

25. Kochenderfer, J.N., Yu, Z., Frasheri, D., Restifo, N.P., and Rosenberg, S.A. (2010). Adoptive transfer of syngeneic T cells transduced with a chimeric antigen receptor that recognizes murine CD19 can eradicate lymphoma and normal B cells. Blood *116*, 3875–3886.

26. Pegram, H.J., Lee, J.C., Hayman, E.G., Imperato, G.H., Tedder, T.F., Sadelain, M., and Brentjens, R.J. (2012). Tumor-targeted T cells modified to secrete IL-12 eradicate systemic tumors without need for prior conditioning. Blood *119*, 4133–4141.

27. Davila, M.L., Kloss, C.C., Gunset, G., and Sadelain, M. (2013). CD19 CAR-targeted T cells induce long-term remission and B Cell Aplasia in an immunocompetent mouse model of B cell acute lymphoblastic leukemia. PLoS ONE *8*, e61338.

28. Brenner, S., Whiting-Theobald, N., Kawai, T., Linton, G.F., Rudikoff, A.G., Choi, U., Ryser, M.F., Murphy, P.M., Sechler, J.M., and Malech, H.L. (2004). CXCR4-transgene expression significantly improves marrow engraftment of cultured hematopoietic stem cells. Stem Cells *22*, 1128–1133.

29. McDermott, D.H., Liu, Q., Ulrick, J., Kwatemaa, N., Anaya-O'Brien, S., Penzak, S.R., Filho, J.O., Priel, D.A., Kelly, C., Garofalo, M., et al. (2011). The CXCR4 antagonist plerixafor corrects panleukopenia in patients with WHIM syndrome. Blood *118*, 4957–4962.

30. Pollock, J.D., Williams, D.A., Gifford, M.A., Li, L.L., Du, X., Fisherman, J., Orkin, S.H., Doerschuk, C.M., and Dinauer, M.C. (1995). Mouse model of X-linked chronic granulomatous disease, an inherited defect in phagocyte superoxide production. Nat. Genet. *9*, 202–209.

31. Vowells, S.J., Sekhsaria, S., Malech, H.L., Shalit, M., and Fleisher, T.A. (1995). Flow cytometric analysis of the granulocyte respiratory burst: a comparison study of fluorescent probes. J. Immunol. Methods *178*, 89–97.

32. Ho, M.S., Medcalf, R.L., Livesey, S.A., and Traianedes, K. (2015). The dynamics of adult haematopoiesis in the bone and bone marrow environment. Br. J. Haematol. *170*, 472–486.

33. Cooper, L.J., Topp, M.S., Serrano, L.M., Gonzalez, S., Chang, W.C., Naranjo, A., Wright, C., Popplewell, L., Raubitschek, A., Forman, S.J., and Jensen, M.C. (2003). T-cell clones can be rendered specific for CD19: toward the selective augmentation of the graft-versus-B-lineage leukemia effect. Blood *101*, 1637–1644.

34. Lee, J.C., Hayman, E., Pegram, H.J., Santos, E., Heller, G., Sadelain, M., and Brentjens, R. (2011). In vivo inhibition of human CD19-targeted effector T cells by natural T regulatory cells in a xenotransplant murine model of B cell malignancy. Cancer Res. *71*, 2871–2881.

35. Nishikawa, T., Miyahara, E., Kurauchi, K., Watanabe, E., Ikawa, K., Asaba, K., Tanabe, T., Okamoto, Y., and Kawano, Y. (2015). Mechanisms of Fatal Cardiotoxicity following High-Dose Cyclophosphamide Therapy and a Method for Its Prevention. PLoS ONE *10*, e0131394.

36. Le, D.T., and Jaffee, E.M. (2012). Regulatory T-cell modulation using cyclophosphamide in vaccine approaches: a current perspective. Cancer Res. *72*, 3439–3444.

37. Weiss, L., Abdul-Hai, A., Or, R., Amir, G., and Polliack, A. (2003). Fludarabine in combination with cyclophosphamide decreases incidence of GVHD and maintains effective graft-versus-leukemia effect after allogeneic stem cell transplantation in murine lymphocytic leukemia. Bone Marrow Transplant. *31*, 11–15.

38. Tomita, Y., Yoshikawa, M., Zhang, Q.W., Shimizu, I., Okano, S., Iwai, T., Yasui, H., and Nomoto, K. (2000). Induction of permanent mixed chimerism and skin allograft tolerance across fully MHC-mismatched barriers by the additional myelosuppressive treatments in mice primed with allogeneic spleen cells followed by cyclophosphamide. J. Immunol. *165*, 34–41.

39. Wu, T., Sozen, H., Luo, B., Heuss, N., Kalscheuer, H., Lan, P., Sutherland, D.E., Hering, B.J., and Guo, Z. (2002). Rapamycin and T cell costimulatory blockade as post-transplant treatment promote fully MHC-mismatched allogeneic bone marrow engraftment under irradiation-free conditioning therapy. Bone Marrow Transplant. *29*, 949–956.

40. Nilsson, C., Forsman, J., Hassan, Z., Abedi-Valugerdi, M., O'Connor, C., Concha, H., Jansson, M., and Hassan, M. (2005). Effect of altering administration order of busulphan and cyclophosphamide on the myeloablative and immunosuppressive properties of the conditioning regimen in mice. Exp. Hematol. *33*, 380–387.

41. Mariotti, J., Taylor, J., Massey, P.R., Ryan, K., Foley, J., Buxhoeveden, N., Felizardo, T.C., Amarnath, S., Mossoba, M.E., and Fowler, D.H. (2011). The pentostatin plus cyclophosphamide nonmyeloablative regimen induces durable host T cell functional deficits and prevents murine marrow allograft rejection. Biol. Blood Marrow Transplant. *17*, 620–631.

42. Nagasawa, T. (2015). CXCL12/SDF-1 and CXCR4. Front. Immunol. *6*, 301.

43. Aiuti, A., Turchetto, L., Cota, M., Cipponi, A., Brambilla, A., Arcelloni, C., Paroni, R., Vicenzi, E., Bordignon, C., and Poli, G. (1999). Human CD34(+) cells express CXCR4 and its ligand stromal cell-derived factor-1. Implications for infection by T-cell tropic human immunodeficiency virus. Blood *94*, 62–73.

44. Miettinen, M., and Lasota, J. (2005). KIT (CD117): a review on expression in normal and neoplastic tissues, and mutations and their clinicopathologic correlation. Appl. Immunohistochem. Mol. Morphol. *13*, 205–220.

45. Hachiya, A., Sriwiriyanont, P., Kobayashi, T., Nagasawa, A., Yoshida, H., Ohuchi, A., Kitahara, T., Visscher, M.O., Takema, Y., Tsuboi, R., and Boissy, R.E. (2009). Stem cell factor-KIT signalling plays a pivotal role in regulating pigmentation in mammalian hair. J. Pathol. *218*, 30–39.

46. Kakarla, S., and Gottschalk, S. (2014). CAR T cells for solid tumors: armed and ready to go? Cancer J. *20*, 151–155.

47. Yu, S., Li, A., Liu, Q., Li, T., Yuan, X., Han, X., and Wu, K. (2017). Chimeric antigen receptor T cells: a novel therapy for solid tumors. J. Hematol. Oncol. *10*, 78.

48. Gargett, T., and Brown, M.P. (2014). The inducible caspase-9 suicide gene system as a "safety switch" to limit on-target, off-tumor toxicities of chimeric antigen receptor T cells. Front. Pharmacol. *5*, 235.

49. Tasian, S.K., Kenderian, S.S., Shen, F., Ruella, M., Shestova, O., Kozlowski, M., Li, Y., Schrank-Hacker, A., Morrissette, J.J.D., Carroll, M., et al. (2017). Optimized depletion of chimeric antigen receptor T cells in murine xenograft models of human acute myeloid leukemia. Blood *129*, 2395–2407.

50. Ogawa, M., Matsuzaki, Y., Nishikawa, S., Hayashi, S., Kunisada, T., Sudo, T., Kina, T., Nakauchi, H., and Nishikawa, S. (1991). Expression and function of c-kit in hemopoietic progenitor cells. J. Exp. Med. *174*, 63–71.

51. Nicholson, I.C., Lenton, K.A., Little, D.J., Decorso, T., Lee, F.T., Scott, A.M., Zola, H., and Hohmann, A.W. (1997). Construction and characterisation of a functional CD19 specific single chain Fv fragment for immunotherapy of B lineage leukaemia and lymphoma. Mol. Immunol. *34*, 1157–1165.

52. Kochenderfer, J.N., Feldman, S.A., Zhao, Y., Xu, H., Black, M.A., Morgan, R.A., Wilson, W.H., and Rosenberg, S.A. (2009). Construction and preclinical evaluation of an anti-CD19 chimeric antigen receptor. J. Immunother. *32*, 689–702.

53. Jacoby, E., Nguyen, S.M., Fountaine, T.J., Welp, K., Gryder, B., Qin, H., Yang, Y., Chien, C.D., Seif, A.E., Lei, H., et al. (2016). CD19 CAR immune pressure induces B-precursor acute lymphoblastic leukaemia lineage switch exposing inherent leukaemic plasticity. Nat. Commun. *7*, 12320.

54. De Ravin, S.S., Wu, X., Moir, S., Anaya-O'Brien, S., Kwatemaa, N., Littel, P., Theobald, N., Choi, U., Su, L., Marquesen, M., et al. (2016). Lentiviral hematopoietic stem cell gene therapy for X-linked severe combined immunodeficiency. Sci. Transl. Med. *8*, 335ra57.

55. D'Hondt, L., Lambert, J.F., Damon, J., Benoit, B.O., Cerny, J., Carlson, J.E., Reilly, J., Wuu, J., Colvin, G.A., Dooner, M.S., and Quesenberry, P.J. (2002). Engraftment of post 5-fluorouracil murine marrow into minimally myeloablated (100 cGy) murine hosts. J. Hematother. Stem Cell Res. *11*, 483–490.

**YMTHE, Volume *26***

## Supplemental Information

# Myeloid Conditioning with c-kit-Targeted CAR-T Cells Enables Donor Stem Cell Engraftment

**Yasuyuki Arai, Uimook Choi, Cristina I. Corsino, Sherry M. Koontz, Masaki Tajima, Colin L. Sweeney, Mary A. Black, Steven A. Feldman, Mary C. Dinauer, and Harry L. Malech**

# Figure S1

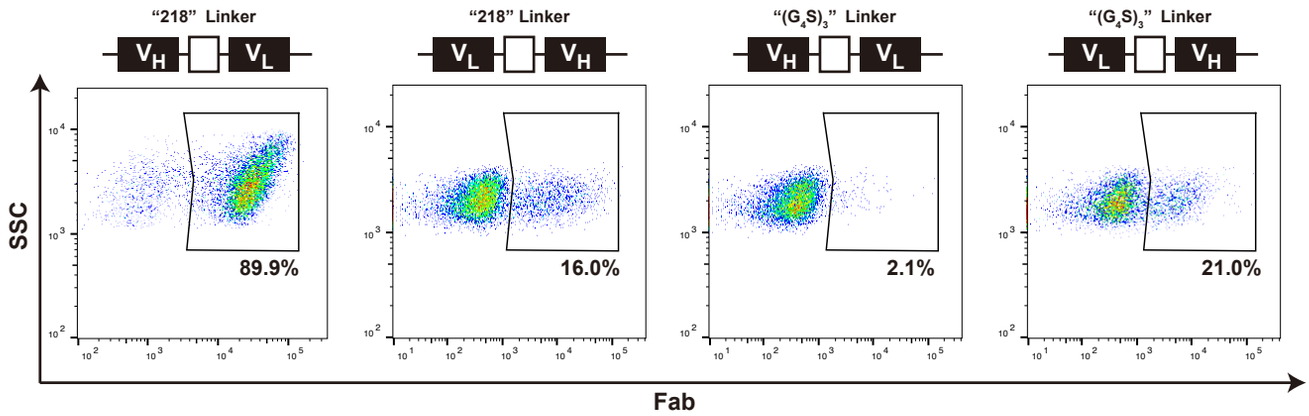


**Effect of linker choice ( "218" versus "$(G_4S)_3$" ) and the $V_H$ and $V_L$ order on CAR expression**

Schematics of four extracellular domain constructs are shown above each FACS dot plot (side scatter by Fab detection) of T cells transduced with versions of c-kit CAR containing the indicated domains.

# Figure S2

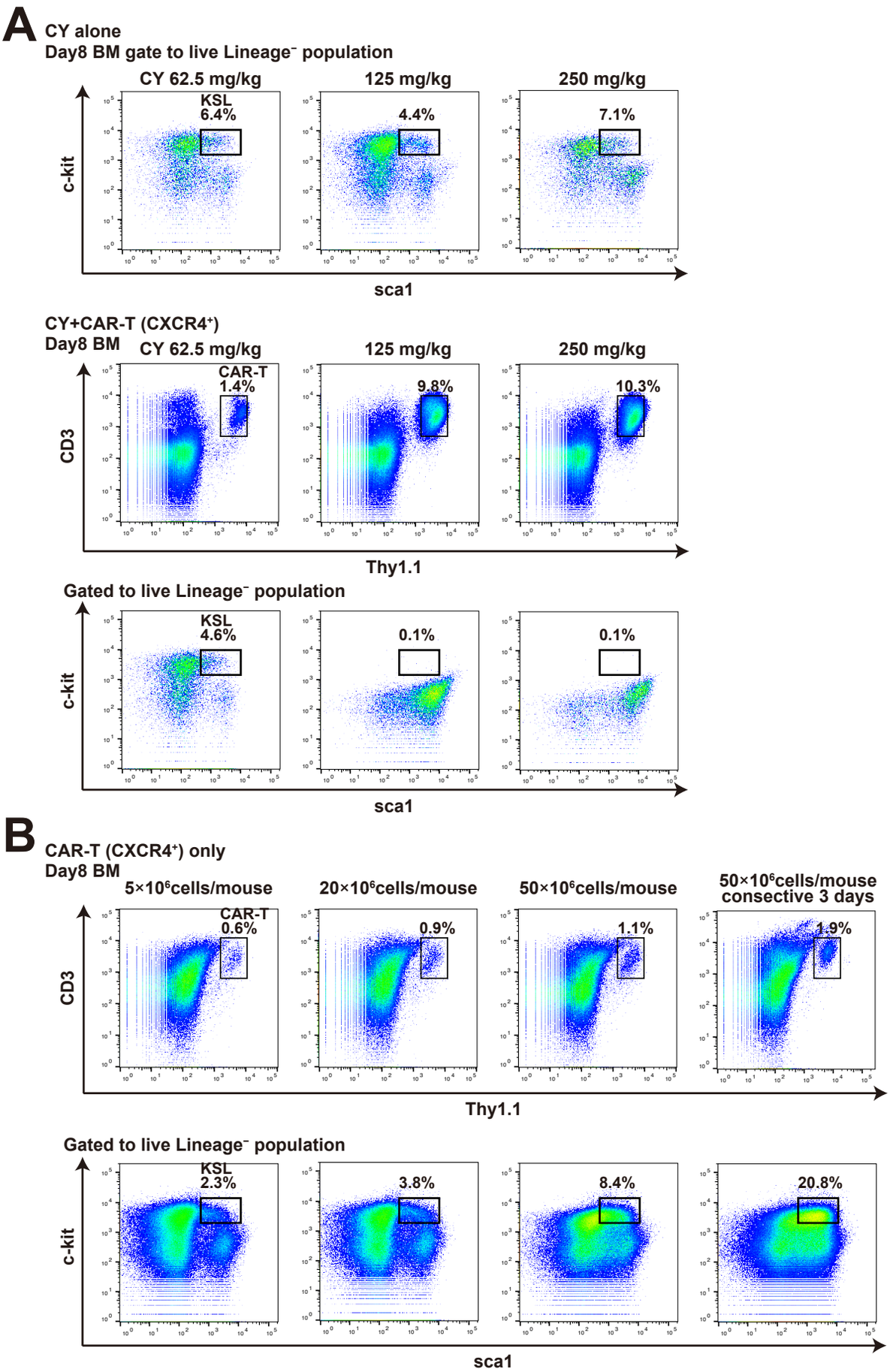


**Dose effect of CY treatment on BM and dose response of CXCR4⁺ c-kit CAR-T cell administration on BM**

**(A)** FACS analyses of CY dose response effect on BM KSL population (upper row), on trafficking of CXCR4⁺ c-kit CAR-T cells to BM (middle row), and on the CXCR4⁺ c-kit CAR-T cells mediated depletion of BM KSL population (lower panel). **(B)** FACS analyses of dose response of CXCR4⁺ c-kit CAR-T cell administration to mice without CY pre-treatment on trafficking of CXCR4⁺ c-kit CAR-T cells to BM (upper panel), and on BM KSL population (lower panel).

# Figure S3

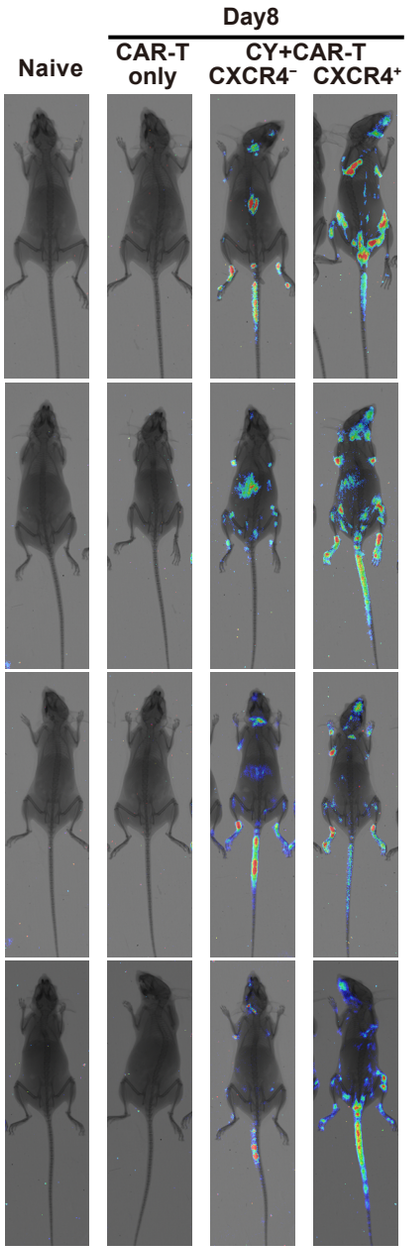


***In vivo* whole body luciferase luminescence imaging**

*In vivo* whole body luciferase luminescence imaging overlaid on X-ray imaging at Day 8 following tail vein injection of transgenic luciferase$^{+}$ Thy1.1 untransduced T cells (naïve), CXCR4$^{-}$ c-kit CAR-T cells without CY pre-treatment (CAR-T only), CXCR4$^{-}$ c-kit CAR-T cells with CY pre-treatment (CY+CAR-T; CXCR4$^{-}$), or CXCR4$^{+}$ c-kit CAR-T cells with CY pre-treatment (CY+CAR-T; CXCR4$^{+}$).

# Figure S4

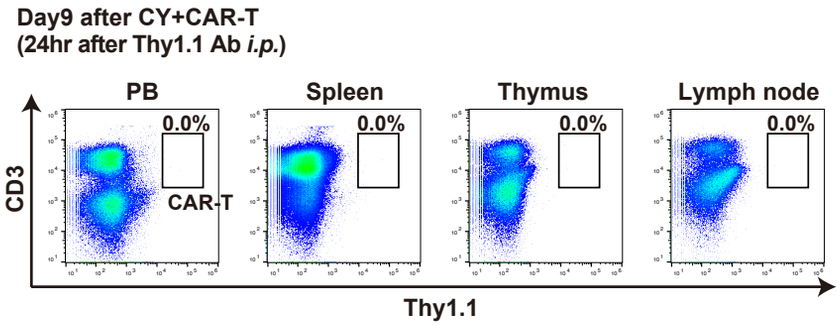


**FACS analysis of residual c-kit CAR-T cells in other organs after anti-Thy1.1 antibody injection**

FACS analysis of congenic Thy1.1$^{+}$ CD45.2$^{+}$ CXCR4$^{+}$ c-kit CAR-T cells in recipient PB, spleen, thymus, and lymph nodes 24 hrs after *i.p.* injection (Day 9 after CY+CAR-T) of anti-Thy1.1 antibody.

# Figure S5

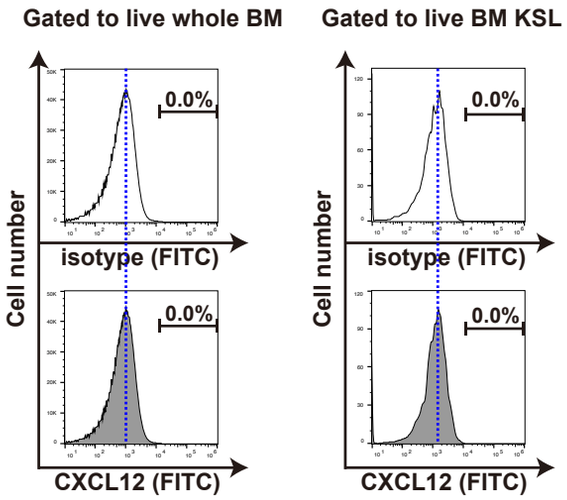


**Expression of CXCL12 (SDF-1, CXCR4 ligand) in mouse whole BM and BM KSL**

FACS analysis of mouse whole BM and BM KSL (c-kit$^{+}$sca1$^{+}$Lineage$^{-}$) for CXCL12 (conjugated with FITC). CXCL12 expression was compared with isotype control.